

From characteristic functions to multivariate distribution functions and European option prices by the (damped) COS method

Gero Junike*, Hauke Stier†

February 17, 2026

Abstract

We provide a unified framework to obtain numerically certain quantities, such as the distribution function, absolute moments and prices of financial options, from the characteristic function of some (unknown) probability density function using the Fourier-cosine series (COS) method. The classical COS method is numerically very efficient in one dimension, but it cannot deal very well with certain integrands in general dimensions. Therefore, we introduce the damped COS method, which can handle a large class of integrands very efficiently. We prove the convergence of the (damped) COS method and study its order of convergence. The method converges exponentially if the characteristic function decays exponentially. To apply the (damped) COS method, one has to specify two parameters: a truncation range for the multivariate density and the number of terms to approximate the truncated density by a Fourier-cosine series. We provide an explicit formula for the truncation range and an implicit formula for the number of terms. Numerical experiments up to five dimensions confirm the theoretical results.

Keywords: Fourier transform, numerical integration, inversion theorem, COS method, CDF, option pricing

Mathematics Subject Classification 65D30 · 65T40 · 65Z05 · 60E10

1 Introduction

We aim to solve the following integral numerically:

$$\int_{\mathbb{R}^d} w(\mathbf{x})g(\mathbf{x})d\mathbf{x}. \quad (1.1)$$

The function g is usually a density and the function w is called *function of interest*. Integrals as in (1.1) appear in a wide range of applications: The integral is equal to the cumulative distribution function (CDF) of the density g if w is an indicator function. CDFs appear in many scientific disciplines.

If w is the absolute value, the integral describes the absolute moment of the density g , which plays an important role in various disciplines but is not easy to obtain, see Von Bahr (1965); Brown (1972); Barndorff-Nielsen and Stelzer (2005) and references therein.

In a financial context, the function w might also describe some financial contract, which depends on several assets. The function g is then the density of the logarithmic returns of the assets and the integral describes the price of the contract.

In many cases, the precise structure of g is unknown, but the Fourier transform \hat{g} is often given in closed form. For example: while the joint density of the sum of two independent random variables can only be expressed as a convolution and is usually not given explicitly, the joint characteristic function is much

*This is a post-peer-review, pre-copyedit version of an article published in SIAM Journal on Numerical Analysis. The final authenticated version is available online at: Junike, G. and Stier, H. (2025). From Characteristic Functions to Multivariate Distribution Functions and European Option Prices by the (Damped) COS Method. SIAM Journal on Numerical Analysis, 63(6), 2421-2453, <https://doi.org/10.1137/24M1666240>

Corresponding author. Department of Mathematics, Ludwig-Maximilians Universität, Theresienstr. 39, 80333 München, Germany. ORCID: 0000-0001-8686-2661, E-mail: gero.junike@math.lmu.de

†Department of Mathematics, Carl von Ossietzky Universität, 26129 Oldenburg, Germany.

simpler to obtain (it is just the product of the marginal characteristic functions). Moreover, the characteristic function of a Lévy process at a particular time-point is usually given explicitly thanks to the Lévy-Khintchine formula.

The integral in (1.1) can be solved numerically using various techniques, including (quasi) Monte Carlo simulation, numerical quadrature and Fourier inversion. Special Fourier-inversion methods exist in the case of a CDF, e.g., the Gil-Pelaez formula, see Gil-Pelaez (1951) and extensions, e.g., Schorr (1975); Waller et al. (1995); Hughett (1998) in one dimension and Shephard (1991a,b) in d dimensions.

The COS method, see Fang and Oosterlee (2009a) for $d = 1$ and Ruijter and Oosterlee (2012) for $d = 2$, is a Fourier inversion technique. The COS method has been applied extensively in computational finance, see Fang and Oosterlee (2009b, 2011); Grzelak and Oosterlee (2011); Zhang and Oosterlee (2013); Leitao et al. (2018); Liu et al. (2019a,b); Oosterlee and Grzelak (2019) and Bardgett et al. (2019).

The COS method has also been applied to solve backward stochastic differential equations, see Ruijter and Oosterlee (2015) and Andersson et al. (2023).

The main ideas of the COS method are to truncate the integration range in (1.1) to some finite hypercube and to approximate the density g on the finite truncation range by a classical Fourier-cosine series. There is a clever trick to approximate the Fourier-cosine coefficients for g in a very fast and robust way using \hat{g} . The COS method is particularly fast when the Fourier-cosine coefficients of the function of interest w are given analytically. However, in multivariate dimensions this is rarely the case an exception being a CDF. For example, the Fourier-cosine coefficients of arithmetic basket options, call-on-minimum and spread options are not given explicitly. Ruijter and Oosterlee (2012) propose in these cases to obtain the Fourier-cosine coefficients of the function of interest numerically by a discrete cosine transform, but this approach slows the COS method significantly. In this article, we introduce the *damped COS method*, which is able to avoid the expensive application of the discrete cosine transform if the Fourier transform of the function of interest is given in closed form. The main idea is to damp w by multiplying it by an exponential function in order to make the damped function of interest integrable. The idea of introducing a damping factor dates back at least to Carr and Madan (1999) and Lewis (2001). In multivariate dimensions, damping is also applied by Eberlein et al. (2010), where the optimal damping factor is determined by Bayer et al. (2023).

Other Fourier techniques to solve integrals as in (1.1) can be found in Carr and Madan (1999); Lewis (2001); Lord et al. (2008); Eberlein et al. (2010); Ortiz-Gracia and Oosterlee (2013); Kirkby (2015); Ortiz-Gracia and Oosterlee (2016); Baschetti et al. (2022) and Bayer et al. (2024).

This article makes the following main contributions: We prove the convergence of the multidimensional classical and damped COS methods, we analyze the order of convergence of the classical and the damped COS methods, and we provide explicit and implicit formulas for the truncation range and the number of terms, respectively. The new approach to finding the number of terms in d dimensions is completely distinct from the one-dimensional case discussed in Junike (2024). Unlike Ruijter and Oosterlee (2012), who analyze the classical COS method, we include in our analysis numerical uncertainty on the characteristic function \hat{g} . This makes it possible to understand how approximations on \hat{g} affect the total error of the COS method.

In one dimension, it is well known that the COS method converges exponentially if the density g is smooth and has semi-heavy tails and performs favorably to the Carr-Madan formula, see Fang and Oosterlee (2009a) and Junike (2024). However, the order of convergence of the COS method is only linear if g has heavy tails, which holds for instance for the stable law. In such cases the Carr-Madan formula outperforms the COS method, see Junike (2024). There are also other methods, such as the SINC method or the PROJ method, which have demonstrated superior performance compared to the COS method in certain scenarios, see Baschetti et al. (2022) and Kirkby (2015).

In multivariate dimensions, the classical COS method becomes slow for many function of interest w , e.g., arithmetic basket options, since the Fourier-cosine coefficients of w need to be approximated numerically. In two dimensions, the classical COS method is significantly slower than the Lewis formula, see Bayer et al. (2023). This disadvantage can be circumvented by the damped COS method introduced in Section 6.4.

The classical and damped COS methods suffer from the curse of dimensionality and are efficient only for moderate dimensions: We show empirically that the COS method outperforms a crude Monte Carlo simulation in $d \in \{2, 3\}$. A Monte Carlo simulation is recommended for $d \geq 5$. The choice between the COS method and a Monte Carlo simulation in $d = 4$ dimensions depends on the required error tolerance and the function of interest. Note that some Fourier inversion approaches are faster than Monte Carlo simulations up to 15 dimensions, see Bayer et al. (2024).

This article is structured as follows: In Section 2 we fix some notation. In Section 3 we introduce the multidimensional classical and damped COS methods, prove its convergence, analyze the order of convergence and provide explicit and implicit formulas for the truncation range and the number of terms. In Section 4 we discuss some examples for g and \widehat{g} . In Section 5 we discuss some functions of interest, i.e., examples for w . In Section 6 we provide numerical experiments. Section 7 concludes.

2 Notation

Let $d \in \mathbb{N}$. Let \mathcal{L}^1 and \mathcal{L}^2 denote the sets of integrable and square-integrable functions from \mathbb{R}^d to \mathbb{R} and by $\langle \cdot, \cdot \rangle$ and $\|\cdot\|_2$ we denote the scalar product and the (semi)norm on \mathcal{L}^2 , respectively. The supremum norm of a function $g : \mathbb{R}^d \rightarrow \mathbb{C}$ is defined by $\|g\|_\infty := \sup_{\mathbf{x} \in \mathbb{R}^d} |g(\mathbf{x})|$. By \mathcal{L}^∞ we denote the set of bounded functions from \mathbb{R}^d to \mathbb{R} . By $\Re\{z\}$ and $\Im\{z\}$ we denote the real and imaginary parts of a complex number $z \in \mathbb{C}$. The complex unit is denoted by i . By Γ , we denote the Gamma function. The Euclidean norm and the maximum norm on \mathbb{R}^d are denoted by $|\cdot|$ and by $|\cdot|_\infty$, respectively. For $\mathbf{x}, \mathbf{y} \in \mathbb{R}^d$ we define

$$\mathbf{x} \geq \mathbf{y} : \Leftrightarrow x_1 \geq y_1, \dots, x_d \geq y_d$$

and treat “ \leq ”, “ $<$ ”, “ $>$ ”, “ $=$ ” and “ \neq ” similarly. We set $\mathbb{R}_+^d := \{\mathbf{x} \in \mathbb{R}^d, \mathbf{x} > \mathbf{0}\}$ and $\mathbb{R}_-^d := \{\mathbf{x} \in \mathbb{R}^d, \mathbf{x} < \mathbf{0}\}$. For $\mathbf{a}, \mathbf{b} \in \mathbb{R}^d$ with $\mathbf{a} \leq \mathbf{b}$, two complex vectors $\mathbf{z}, \mathbf{y} \in \mathbb{C}^d$ and $\lambda \in \mathbb{C}$ we define $\mathbf{z} + \mathbf{y} := (z_1 + y_1, \dots, z_d + y_d) \in \mathbb{C}^d$ and treat $\mathbf{z}\mathbf{y}$ and $\frac{\mathbf{z}}{\mathbf{y}}$ similarly. We further define

$$\begin{aligned} \mathbf{z} \cdot \mathbf{y} &:= z_1 y_1 + \dots + z_d y_d \in \mathbb{C} \\ \lambda \mathbf{z} &:= (\lambda z_1, \dots, \lambda z_d) \in \mathbb{C}^d \\ [\mathbf{a}, \mathbf{b}] &:= [a_1, b_1] \times \dots \times [a_d, b_d] \subset \mathbb{R}^d \\ (-\infty, \mathbf{b}] &:= (-\infty, b_1] \times \dots \times (-\infty, b_d] \subset \mathbb{R}^d \\ \exp(\mathbf{x}) &:= (\exp(x_1), \dots, \exp(x_d)) \in \mathbb{R}^d, \quad \mathbf{x} \in \mathbb{R}^d \\ \log(\mathbf{x}) &:= (\log(x_1), \dots, \log(x_d)) \in \mathbb{R}^d, \quad \mathbf{x} \in \mathbb{R}_+^d. \end{aligned}$$

For a subset $A \subset \mathbb{R}^d$, we define the indicator function $1_A(\mathbf{x})$ by one if $\mathbf{x} \in A$ and by zero otherwise. Let $\mathbb{N}_0 = \mathbb{N} \cup \{0\}$. For $\mathbf{N} = (N_1, \dots, N_d) \in \mathbb{N}_0^d$ and a sequence $(a_{\mathbf{k}})_{\mathbf{k} \in \mathbb{N}_0^d} \subset \mathbb{C}$, we define

$$\sum'_{\mathbf{0} \leq \mathbf{k} \leq \mathbf{N}} a_{\mathbf{k}} := \sum_{\mathbf{0} \leq \mathbf{k} \leq \mathbf{N}} \frac{1}{2^{\Lambda(\mathbf{k})}} a_{\mathbf{k}},$$

where $\Lambda(\mathbf{k})$ is the number of components of the vector \mathbf{k} that are equal to zero, i.e., $\Lambda(\mathbf{k}) := \sum_{h=1}^d 1_{\{0\}}(k_h)$. For an integrable function $\psi : \mathbb{R}^d \rightarrow \mathbb{C}$ we define its *Fourier transform* by

$$\widehat{\psi}(\mathbf{u}) := \int_{\mathbb{R}^d} \psi(\mathbf{x}) e^{i\mathbf{u} \cdot \mathbf{x}} d\mathbf{x}, \quad \mathbf{u} \in \mathbb{R}^d. \quad (2.1)$$

This definition of the Fourier transform also appears in Bauer (1996, Def. 22.6) and in Eberlein et al. (2010). Provided the integral in (2.1) exists, the domain of $\widehat{\psi}$ may also be extended to parts of the complex plane. If $\psi \geq 0$ and $\int \psi(\mathbf{x}) d\mathbf{x} = 1$, then ψ is called *density*, $\widehat{\psi}$ is called the *characteristic function* and the map $\mathbf{y} \mapsto \int_{(-\infty, \mathbf{y}]} \psi(\mathbf{x}) d\mathbf{x}$ is called the *cumulative distribution function* (CDF).

The next definition introduces the concept of *COS-admissibility* and extends Junike and Pankrashkin (2022, Def. 1) to the multidimensional setting. It is necessary to prove the convergence of the COS method.

Definition 2.1. Let $\mathbf{L} = (L_1, \dots, L_d) \in \mathbb{R}_+^d$. A function $\psi \in \mathcal{L}^1$ is called *COS-admissible* if

$$B_\psi(\mathbf{L}) := \sum'_{\mathbf{k} \in \mathbb{N}_0^d} \frac{1}{\prod_{h=1}^d L_h} \left| \int_{\mathbb{R}^d \setminus [-\mathbf{L}, \mathbf{L}]} \psi(\mathbf{x}) e_{\mathbf{k}}(\mathbf{x}) d\mathbf{x} \right|^2 \rightarrow 0, \quad \min_{h=1, \dots, d} L_h \rightarrow \infty.$$

The functions $e_{\mathbf{k}}$ are defined in Equation (3.9). If a function $\psi \in \mathcal{L}^1 \cap \mathcal{L}^2$ satisfies

$$\int_{\mathbb{R}^d} |\mathbf{x}|^{2d} |\psi(\mathbf{x})|^2 d\mathbf{x} < \infty, \quad (2.2)$$

then ψ is COS-admissible, see Proposition A.1 in the appendix. In particular, it follows that bounded densities with existing moments satisfy Inequality (2.2).

Remark 2.2. In one dimension, there are other sufficient conditions than Inequality (2.2) to ensure COS-admissibility, see Junike and Pankrashkin (2022, Corollary 4) and Junike (2024, Lemma 3.7).

Junike and Pankrashkin (2022) and Junike (2024) assume that g has semi-heavy tails, i.e., g decays exponentially or faster. Here, we make the same assumption in multivariate dimensions in order to be able to estimate the truncation range and the number of terms of the COS method.

Definition 2.3. We say a function $\psi : \mathbb{R}^d \rightarrow \mathbb{R}$ decays exponentially if there are $C_1, C_2, m > 0$ such that for $|\mathbf{x}| > m$ it holds that $|\psi(\mathbf{x})| \leq C_1 e^{-C_2 |\mathbf{x}|}$.

We denote the set of functions from \mathbb{R}^d to \mathbb{R} which decay exponentially and satisfy Inequality (2.2) by \mathcal{L}^e .

3 Classical and damped COS methods

Problem statement: Throughout the paper, we fix a density $g : \mathbb{R}^d \rightarrow \mathbb{R}$ and a function of interest $w : \mathbb{R}^d \rightarrow \mathbb{R}$. We aim to solve the integral in (1.1) numerically.

Typically, for the function of interest, it holds that $w \notin \mathcal{L}^1$. For example, the integral in (1.1) is equal to the CDF of g evaluated at $\mathbf{y} \in \mathbb{R}^d$ if $w(\mathbf{x}) = 1_{(-\infty, \mathbf{y}]}$ for $\mathbf{x} \in \mathbb{R}^d$. Or, in a financial context, an unweighted arithmetic basket put option is defined by $w(\mathbf{x}) = \max(K - \sum_{h=1}^d e^{x_h}, 0)$, $\mathbf{x} \in \mathbb{R}^d$, where $K > 0$, see e.g., Bayer et al. (2023).

Note that for many densities and functions of interest, both \hat{g} and \hat{w} are given in closed form, see e.g., Ruijter and Oosterlee (2012); Eberlein et al. (2010) and references therein. The density g does not need to be known precisely to apply the classical or the damped COS method. Let $\boldsymbol{\alpha} \in \mathbb{R}^d$ be a damping factor. Let

$$\delta_g := \{ \boldsymbol{\alpha} \in \mathbb{R}^d : \mathbf{x} \mapsto g(\mathbf{x})e^{\boldsymbol{\alpha} \cdot \mathbf{x}} \in \mathcal{L}^1 \cap \mathcal{L}^2 \cap \mathcal{L}^e \} \quad (3.1)$$

$$\delta_w^\infty := \{ \boldsymbol{\alpha} \in \mathbb{R}^d : \mathbf{x} \mapsto w(\mathbf{x})e^{-\boldsymbol{\alpha} \cdot \mathbf{x}} \in \mathcal{L}^\infty \} \quad (3.2)$$

$$\delta_w := \{ \boldsymbol{\alpha} \in \mathbb{R}^d : \mathbf{x} \mapsto w(\mathbf{x})e^{-\boldsymbol{\alpha} \cdot \mathbf{x}} \in \mathcal{L}^1 \cap \mathcal{L}^2 \cap \mathcal{L}^e \cap \mathcal{L}^\infty \}. \quad (3.3)$$

The following Assumption A1 is a sufficient condition to prove the convergence of the classical COS method and Assumption A2 is a sufficient condition to prove the convergence of the damped COS method.

Assumption A1. We assume that $\delta_g \cap \delta_w^\infty \neq \emptyset$ and $\boldsymbol{\alpha} \in \delta_g \cap \delta_w^\infty$.

Assumption A2. We assume that $\delta_g \cap \delta_w \neq \emptyset$ and $\boldsymbol{\alpha} \in \delta_g \cap \delta_w$.

Assume Assumption A1 or A2 holds. It holds that $wg \in \mathcal{L}^1$ since w is bounded and g is a density. For a scaling factor $\lambda > 0$ and a shift parameter $\boldsymbol{\mu} \in \mathbb{R}^d$, we define the *damped density* by

$$f(\mathbf{x}) = \lambda e^{\boldsymbol{\alpha} \cdot (\mathbf{x} + \boldsymbol{\mu})} g(\mathbf{x} + \boldsymbol{\mu}), \quad \mathbf{x} \in \mathbb{R}^d \quad (3.4)$$

and the *damped function of interest* by

$$v(\mathbf{x}) = \frac{1}{\lambda} e^{-\boldsymbol{\alpha} \cdot (\mathbf{x} + \boldsymbol{\mu})} w(\mathbf{x} + \boldsymbol{\mu}), \quad \mathbf{x} \in \mathbb{R}^d. \quad (3.5)$$

By definition, it follows that

$$\int_{\mathbb{R}^d} w(\mathbf{x})g(\mathbf{x})d\mathbf{x} = \int_{\mathbb{R}^d} v(\mathbf{x})f(\mathbf{x})d\mathbf{x}. \quad (3.6)$$

Remark 3.1. By Proposition A.2 it holds that $\widehat{f}(\mathbf{u}) = \lambda e^{-i\mathbf{u}\cdot\boldsymbol{\mu}}\widehat{g}(\mathbf{u} - i\boldsymbol{\alpha})$, i.e., \widehat{f} is given in closed form if \widehat{g} is given in closed form. The Fourier transform of v is given by $\widehat{v}(\mathbf{u}) = \lambda^{-1}e^{-i\mathbf{u}\cdot\boldsymbol{\mu}}\widehat{w}(\mathbf{u} + i\boldsymbol{\alpha})$. Hence, a closed form expression for \widehat{w} is sufficient to obtain a closed form expression for \widehat{v} .

Remark 3.2. Under Assumption A1 or Assumption A2 it holds that $vf \in \mathcal{L}^1$, $f \in \mathcal{L}^1 \cap \mathcal{L}^2 \cap \mathcal{L}^e$ and $v \in \mathcal{L}^\infty$. Under Assumption A2 it holds *additionally* that $v \in \mathcal{L}^1 \cap \mathcal{L}^2 \cap \mathcal{L}^e$.

Remark 3.3. On the choice of λ : In some applications it might be useful to know that g and f are densities. Thanks to Proposition A.2, f is a density if g is a density and if we choose $\lambda = (\widehat{g}(-i\boldsymbol{\alpha}))^{-1}$. If $\boldsymbol{\alpha} = \mathbf{0}$ it holds that $\lambda = 1$.

Remark 3.4. On the choice of $\boldsymbol{\mu}$: to apply the COS method, we need to truncate the density $\mathbf{x} \mapsto \lambda e^{\boldsymbol{\alpha}\cdot\mathbf{x}}g(\mathbf{x})$, i.e., we need to find some interval $[\mathbf{a}, \mathbf{b}]$ such that $\lambda e^{\boldsymbol{\alpha}\cdot\mathbf{x}}g(\mathbf{x}) \approx \lambda e^{\boldsymbol{\alpha}\cdot\mathbf{x}}g(\mathbf{x})1_{[\mathbf{a}, \mathbf{b}]}(\mathbf{x})$. Assume that such an interval is given. Let $\boldsymbol{\mu} := \frac{\mathbf{b}-\mathbf{a}}{2} + \mathbf{a}$ and $\mathbf{L} := \frac{\mathbf{b}-\mathbf{a}}{2}$. Define f as in Equation (3.4). We then have $f \approx f1_{[-\mathbf{L}, \mathbf{L}]}$. Therefore, we can always work with f instead of g and a symmetric interval $[-\mathbf{L}, \mathbf{L}]$ to keep the notation simple. We recall ideas from the literature, how such interval $[\mathbf{a}, \mathbf{b}]$ can be defined: Fang and Oosterlee (2009a, Eq. (49)) and Ruijter and Oosterlee (2012, Eq. (5.8)) suggest setting $[a_h, b_h] := [\int_{\mathbb{R}^d} \lambda e^{\boldsymbol{\alpha}\cdot\mathbf{x}}g(\mathbf{x})x_h d\mathbf{x} \pm L_h]$ for L_h large enough, $h = 1, \dots, d$. We follow this idea and set

$$\mu_h := \frac{b_h - a_h}{2} + a_h = \int_{\mathbb{R}^d} \lambda e^{\boldsymbol{\alpha}\cdot\mathbf{x}}g(\mathbf{x})x_h d\mathbf{x}, \quad h = 1, \dots, d.$$

The vector $\boldsymbol{\mu}$ is equal to the first moments of the marginal densities of $\mathbf{x} \mapsto \lambda e^{\boldsymbol{\alpha}\cdot\mathbf{x}}g(\mathbf{x})$. Proposition A.2 explains how to obtain $\boldsymbol{\mu}$ from \widehat{g} .

Remark 3.5. In some applications, \widehat{g} is not given explicitly but needs to be approximated numerically; e.g., in Duffie et al. (2003), \widehat{g} is the solution to some ordinary differential equation (ODE), which itself needs to be solved numerically before solving the integral (1.1). We denote the approximation of \widehat{g} by ϕ . The corresponding approximation of \widehat{f} is denoted by $\vartheta(\mathbf{u}) := \lambda e^{-i\mathbf{u}\cdot\boldsymbol{\mu}}\phi(\mathbf{u} - i\boldsymbol{\alpha})$, $\mathbf{u} \in \mathbb{R}^d$. We assume that $\phi(\mathbf{u} - i\boldsymbol{\alpha})$ exists for $\mathbf{u} \in \mathbb{R}^d$ to ensure that ϑ is well defined. We have to evaluate \widehat{f} at finitely many points to apply the COS method. So for any fixed $\mathbf{u} \in \mathbb{R}^d$ and any $\delta > 0$ we assume that we can choose ϑ such that $|\widehat{f}(\mathbf{u}) - \vartheta(\mathbf{u})| < \delta$. For example, if ϑ is obtained by the Euler method, the global error between $\widehat{f}(\mathbf{u})$ and $\vartheta(\mathbf{u})$ decreases linearly in the step size for discretization of the ODE, see Section 6.1 for details.

From now on, we will work with \widehat{f} and v instead of \widehat{g} and w . A numerical approximation of \widehat{f} is denoted by a function $\vartheta : \mathbb{R}^d \rightarrow \mathbb{C}$. If there is no numerical uncertainty on \widehat{f} , replace ϑ by \widehat{f} in the rest of the article.

	Aim: Approximate $\int_{\mathbb{R}^d} w(\mathbf{x})g(\mathbf{x})d\mathbf{x}$ by $\sum' \tilde{c}_{\mathbf{k}}v_{\mathbf{k}}$ or by $\sum' \tilde{c}_{\mathbf{k}}\tilde{v}_{\mathbf{k}}$.
$w : \mathbb{R}^d \rightarrow \mathbb{R}$	Function of interest
$g : \mathbb{R}^d \rightarrow \mathbb{R}$	Density function
$\boldsymbol{\alpha}, \boldsymbol{\mu} \in \mathbb{R}^d, \lambda \in \mathbb{R}_+^d$	Damping factor, shift parameter and scaling factor
$v : \mathbb{R}^d \rightarrow \mathbb{R}$	Damped function of interest
$f : \mathbb{R}^d \rightarrow \mathbb{R}$	Damped density function
$\hat{w}, \hat{g}, \hat{v}, \hat{f} : \mathbb{R}^d \rightarrow \mathbb{C}$	Fourier transforms of w, g, v and f
$\phi : \mathbb{R}^d \rightarrow \mathbb{C}$	Numerical approximation of \hat{g}
$\vartheta : \mathbb{R}^d \rightarrow \mathbb{C}$	Numerical approximation of \hat{f}
$e_{\mathbf{k}} : \mathbb{R}^d \rightarrow \mathbb{R}$	Cosine basis functions, see Eq. (3.9)
$\mathbf{L}, \mathbf{M} \in \mathbb{R}_+^d$	Truncation ranges for f and v
$\mathbf{N} \in \mathbb{N}^d$	Number of terms
$\mathbf{0} \leq \mathbf{k} \leq \mathbf{N}$	Index
$a_{\mathbf{k}} \in \mathbb{R}$	Classical Fourier-cosine coefficients of $f1_{[-\mathbf{L}, \mathbf{L}]}$
$c_{\mathbf{k}} \in \mathbb{R}$	Approximation of $a_{\mathbf{k}}$ through \hat{f} , see Eq. (3.11)
$\tilde{c}_{\mathbf{k}} \in \mathbb{R}$	Approximation of $c_{\mathbf{k}}$ through ϑ , see Eq. (3.12)
$v_{\mathbf{k}} \in \mathbb{R}$	(Scaled) Fourier-cosine coefficients of $v1_{[-\mathbf{M}, \mathbf{M}]}$, see Eq. (3.14)
$v_{\mathbf{k}}^{\text{Num}} \in \mathbb{R}$	Numerical approximation of $v_{\mathbf{k}}$
$\tilde{v}_{\mathbf{k}} \in \mathbb{R}$	Approximation of $v_{\mathbf{k}}$ through \hat{v} , see Eq. (3.16)
\mathcal{S}	Index set, see Eq. (3.13)
$\mathcal{U}(\mathbf{L}, \mathbf{N})$	Set where \hat{f} needs to be evaluated, see Eq. (3.17).

Table 1: Overview of the multidimensional COS method.

We describe the COS method in detail in order to approximate the right-hand side of Equation (3.6). Table 1 provides an overview. Let $\mathbf{M} \in \mathbb{R}_+^d$ be large enough so that

$$\int_{\mathbb{R}^d} v(\mathbf{x})f(\mathbf{x})d\mathbf{x} \approx \int_{[-\mathbf{M}, \mathbf{M}]} v(\mathbf{x})f(\mathbf{x})d\mathbf{x}. \quad (3.7)$$

Under Assumption A1 or A2, such \mathbf{M} exists since then $vf \in \mathcal{L}^1$. Let $\mathbf{L} \geq \mathbf{M}$. We truncate f on $[-\mathbf{L}, \mathbf{L}]$ and approximate the truncated damped density using a Fourier-cosine series. We intuitively have that

$$f \approx f1_{[-\mathbf{L}, \mathbf{L}]} \approx \sum'_{\mathbf{0} \leq \mathbf{k} \leq \mathbf{N}} a_{\mathbf{k}}e_{\mathbf{k}}1_{[-\mathbf{L}, \mathbf{L}]} \approx \sum'_{\mathbf{0} \leq \mathbf{k} \leq \mathbf{N}} c_{\mathbf{k}}e_{\mathbf{k}}1_{[-\mathbf{L}, \mathbf{L}]} \approx \sum'_{\mathbf{0} \leq \mathbf{k} \leq \mathbf{N}} \tilde{c}_{\mathbf{k}}e_{\mathbf{k}}1_{[-\mathbf{L}, \mathbf{L}]}, \quad (3.8)$$

where the basis functions are defined by

$$e_{\mathbf{k}}(\mathbf{x}) = \prod_{h=1}^d \cos\left(k_h \pi \frac{x_h + L_h}{2L_h}\right), \quad \mathbf{x} \in \mathbb{R}^d, \quad \mathbf{k} \in \mathbb{N}_0^d \quad (3.9)$$

and the classical Fourier-cosine coefficients (see Pivato (2010, Part III, Section 9)) of $f1_{[-\mathbf{L}, \mathbf{L}]}$ are given for $\mathbf{k} \in \mathbb{N}_0^d$ by

$$\begin{aligned} a_{\mathbf{k}} &= \frac{1}{\prod_{h=1}^d L_h} \int_{[-\mathbf{L}, \mathbf{L}]} f(\mathbf{x})e_{\mathbf{k}}(\mathbf{x})d\mathbf{x} \\ &\approx \frac{1}{\prod_{h=1}^d L_h} \int_{\mathbb{R}^d} f(\mathbf{x})e_{\mathbf{k}}(\mathbf{x})d\mathbf{x} \end{aligned} \quad (3.10)$$

$$= \frac{1}{2^{d-1} \prod_{h=1}^d L_h} \sum_{\mathbf{s} \in \mathcal{S}} \Re \left\{ \hat{f} \left(\frac{\pi}{2} \frac{\mathbf{s}\mathbf{k}}{\mathbf{L}} \right) \exp \left(i \frac{\pi}{2} \mathbf{s} \cdot \mathbf{k} \right) \right\} =: c_{\mathbf{k}} \quad (3.11)$$

$$\approx \frac{1}{2^{d-1} \prod_{h=1}^d L_h} \sum_{\mathbf{s} \in \mathcal{S}} \Re \left\{ \vartheta \left(\frac{\pi}{2} \frac{\mathbf{s}\mathbf{k}}{\mathbf{L}} \right) \exp \left(i \frac{\pi}{2} \mathbf{s} \cdot \mathbf{k} \right) \right\} =: \tilde{c}_{\mathbf{k}}, \quad (3.12)$$

where

$$\mathcal{S} := \{s \in \mathbb{Z}^d : s_1 = 1, s_h \in \{-1, 1\}, h = 2, \dots, d\}. \quad (3.13)$$

The key insight of the COS method is the fact that the integral at the right-hand side of Equation (3.10) can be solved explicitly¹. If \hat{f} needs to be approximated by some function ϑ , we use $\tilde{c}_{\mathbf{k}}$ instead of $c_{\mathbf{k}}$, compare with Remark 3.5.

The idea of the multidimensional COS method is to approximate f as in (3.8), and hence the right-hand side of Equation (3.7) by

$$\int_{[-M, M]} v(\mathbf{x}) f(\mathbf{x}) d\mathbf{x} \approx \sum'_{\mathbf{0} \leq \mathbf{k} \leq \mathbf{N}} \tilde{c}_{\mathbf{k}} \underbrace{\int_{[-M, M]} v(\mathbf{x}) e_{\mathbf{k}}(\mathbf{x}) d\mathbf{x}}_{=: v_{\mathbf{k}}}. \quad (3.14)$$

We summarize from the literature three approaches to computing $v_{\mathbf{k}}$ and propose a new method as well:

COS-i Classical COS method (see Fang and Oosterlee (2009a)): it is assumed that $\alpha = \mathbf{0}$, $v_{\mathbf{k}}$ can be obtained explicitly and that Assumption A1 holds. Examples, where $v_{\mathbf{k}}$ are given analytically, include, in one dimension, plain vanilla put and call options and digital options, see Fang and Oosterlee (2009a) and, in two dimensions, geometric basket options, call-on-maximum options and put-on-minimum options, see Ruijter and Oosterlee (2012). In general dimensions, the coefficients $v_{\mathbf{k}}$ of a CDF are given in closed form, see Example 5.1.

COS-ii Classical COS method approximating $v_{\mathbf{k}}$ numerically (see Ruijter and Oosterlee (2012)): it is assumed that $\alpha = \mathbf{0}$ and that Assumption A1 holds. This method has been applied in cases in which the coefficients $v_{\mathbf{k}}$ cannot be obtained explicitly, e.g. in the case of arithmetic basket options, call-on-minimum and spread options. The coefficients $v_{\mathbf{k}}$ are then approximated numerically by the discrete cosine transform or some quadrature rule. However, solving the integral at the right-hand side of (3.14) numerically for each \mathbf{k} is expensive and slows down the COS method significantly. Let us denote the numerical approximation of $v_{\mathbf{k}}$ by $v_{\mathbf{k}}^{\text{Num}}$.

COS-iii Classical COS method with damping (see Wang (2017)): it is assumed that $\alpha \neq \mathbf{0}$ and $v_{\mathbf{k}}$ can be obtained explicitly and that Assumption A1 holds. Wang (2017) introduces damping (in one dimension) to make the COS method numerically more stable for unbounded functions of interest. We propose to approximate the L_1 -norm by this method in Example 5.4. However, the coefficients $v_{\mathbf{k}}$ (with or without damping) are not given in closed form for many functions of interest, e.g., arithmetic basket options, call-on-minimum and spread options.

COS-iv Damped COS method (new to the literature): it is assumed that $\alpha \neq \mathbf{0}$, \hat{v} is given explicitly and Assumption A2 holds. The coefficients $v_{\mathbf{k}}$ are approximated by $\tilde{v}_{\mathbf{k}}$, which are defined explicitly in terms of \hat{v} in Equation (3.16). This method is much faster than the classical COS method described in COS-ii since the coefficients $\tilde{v}_{\mathbf{k}}$ are given explicitly while $v_{\mathbf{k}}^{\text{Num}}$ are obtained numerically.

The novel damped COS-iv method is defined as follows: assume that Assumption A2 holds, which implies that $v \in \mathcal{L}^1$. Hence, the integral over the finite interval $[-M, M]$ at the right-hand side of (3.14) can be approximated by an integral over \mathbb{R}^d and we approximate the right-hand side of Equation (3.7) by

$$\int_{[-M, M]} v(\mathbf{x}) f(\mathbf{x}) d\mathbf{x} \approx \sum'_{\mathbf{0} \leq \mathbf{k} \leq \mathbf{N}} \tilde{c}_{\mathbf{k}} \underbrace{\int_{\mathbb{R}^d} v(\mathbf{x}) e_{\mathbf{k}}(\mathbf{x}) d\mathbf{x}}_{=: \tilde{v}_{\mathbf{k}}}. \quad (3.15)$$

This works if M is large enough. Similar to the solution presented in Equation (3.11), the coefficients $\tilde{v}_{\mathbf{k}}$ are given analytically:

$$\tilde{v}_{\mathbf{k}} = \frac{1}{2^{d-1}} \sum_{s \in \mathcal{S}} \Re \left\{ \hat{v} \left(\frac{\pi s \mathbf{k}}{2L} \right) \exp \left(i \frac{\pi}{2} s \cdot \mathbf{k} \right) \right\}, \quad (3.16)$$

¹We use $\prod_{h=1}^d \cos \theta_h = \frac{1}{2^{d-1}} \sum_{s \in \mathcal{S}} \cos(s \cdot \theta)$, $\theta \in \mathbb{R}^d$, which follows by mathematical induction, from the fact that the cosine is an even function and from the trigonometric identities stated in Abramowitz and Stegun (1972, Eqs. (4.3.17, 4.3.31)).

provided \widehat{v} is known. As shown in Section 5, there are many functions of interest such that \widehat{v} is given explicitly.

Remark 3.6. In the special case that \widehat{f} only takes real values, the computational cost of the classical COS-i and the damped COS-iv methods can be reduced by (about) a factor of one half, since $c_{\mathbf{k}} = 0$ if $\sum_{h=1}^d k_h$ is odd. This applies for example in the case of the multivariate normal distribution, see Example 4.1.

The following theorem shows that multivariate densities can be approximated by a Fourier-cosine series. The theorem also includes numerical uncertainty on the Fourier transform \widehat{f} . Note that the classical COS-i and the damped COS-iv methods need to evaluate \widehat{f} only at finitely many points, see Equation (3.11), given by

$$\mathcal{U}(\mathbf{L}, \mathbf{N}) := \left\{ \frac{\pi}{2} \frac{\mathbf{s}\mathbf{k}}{\mathbf{L}} : \mathbf{0} \leq \mathbf{k} \leq \mathbf{N}, \mathbf{s} \in \mathcal{S} \right\}. \quad (3.17)$$

Theorem 3.7. (COS approximation of f). *Assume that Assumption A1 or A2 holds. Let $\vartheta : \mathbb{R}^d \rightarrow \mathbb{C}$ and define $\tilde{c}_{\mathbf{k}}$ as in Equation (3.12). For any $\varepsilon > 0$ there exists a $\mathbf{L} \in \mathbb{R}_+^d$, a $\mathbf{N} \in \mathbb{N}^d$ and a $\delta > 0$ such that $\max_{\mathbf{u} \in \mathcal{U}(\mathbf{L}, \mathbf{N})} \left| \widehat{f}(\mathbf{u}) - \vartheta(\mathbf{u}) \right| < \delta$ implies*

$$\left\| f - \sum'_{\mathbf{0} \leq \mathbf{k} \leq \mathbf{N}} \tilde{c}_{\mathbf{k}} e_{\mathbf{k}} 1_{[-\mathbf{L}, \mathbf{L}]} \right\|_2 < \varepsilon.$$

Note that \mathbf{N} depends on \mathbf{L} and that δ depends on both \mathbf{L} and \mathbf{N} .

Proof. Define $e_{\mathbf{k}}^{\mathbf{L}} = e_{\mathbf{k}} 1_{[-\mathbf{L}, \mathbf{L}]}$. It holds for $\mathbf{l}, \mathbf{k} \in \mathbb{N}_0^d$ that

$$\langle e_{\mathbf{k}}^{\mathbf{L}}, e_{\mathbf{l}}^{\mathbf{L}} \rangle = \begin{cases} 2^{\Lambda(\mathbf{k})} \prod_{h=1}^d L_h & , \mathbf{k} = \mathbf{l}, \\ 0 & , \text{otherwise,} \end{cases} \quad (3.18)$$

where Λ is defined in Section 2. For any $\mathbf{L} \in \mathbb{R}_+^d$ and $\mathbf{N} \in \mathbb{N}^d$, it holds that

$$\begin{aligned} \left\| f - \sum'_{\mathbf{0} \leq \mathbf{k} \leq \mathbf{N}} \tilde{c}_{\mathbf{k}} e_{\mathbf{k}}^{\mathbf{L}} \right\|_2 &\leq \underbrace{\|f - f 1_{[-\mathbf{L}, \mathbf{L}]} \|_2}_{=: A_1(\mathbf{L})} + \underbrace{\left\| f 1_{[-\mathbf{L}, \mathbf{L}]} - \sum'_{\mathbf{0} \leq \mathbf{k} \leq \mathbf{N}} a_{\mathbf{k}} e_{\mathbf{k}}^{\mathbf{L}} \right\|_2}_{=: A_2(\mathbf{L}, \mathbf{N})} \\ &+ \underbrace{\left\| \sum'_{\mathbf{0} \leq \mathbf{k} \leq \mathbf{N}} (a_{\mathbf{k}} - c_{\mathbf{k}}) e_{\mathbf{k}}^{\mathbf{L}} \right\|_2}_{=: A_3(\mathbf{L}, \mathbf{N})} + \underbrace{\left\| \sum'_{\mathbf{0} \leq \mathbf{k} \leq \mathbf{N}} (c_{\mathbf{k}} - \tilde{c}_{\mathbf{k}}) e_{\mathbf{k}}^{\mathbf{L}} \right\|_2}_{=: A_4(\mathbf{L}, \mathbf{N})}. \end{aligned}$$

Further,

$$A_3(\mathbf{L}, \mathbf{N})^2 = \sum_{\mathbf{0} \leq \mathbf{k} \leq \mathbf{N}} \sum_{\mathbf{0} \leq \mathbf{l} \leq \mathbf{N}} \frac{1}{2^{\Lambda(\mathbf{k}) + \Lambda(\mathbf{l})}} (a_{\mathbf{k}} - c_{\mathbf{k}})(a_{\mathbf{l}} - c_{\mathbf{l}}) \langle e_{\mathbf{k}}^{\mathbf{L}}, e_{\mathbf{l}}^{\mathbf{L}} \rangle \leq \sum'_{\mathbf{k} \in \mathbb{N}_0^d} \prod_{h=1}^d \{L_h\} |a_{\mathbf{k}} - c_{\mathbf{k}}|^2 = B_f(\mathbf{L}),$$

see Definition 2.1. For $\varepsilon > 0$, choose $\mathbf{L} \in \mathbb{R}_+^d$ such that $A_1(\mathbf{L}) < \frac{\varepsilon}{4}$ and $B_f(\mathbf{L}) < \left(\frac{\varepsilon}{4}\right)^2$. Hence, $A_3(\mathbf{L}, \mathbf{N}) < \frac{\varepsilon}{4}$. Then choose $\mathbf{N} \in \mathbb{N}^d$ such that $A_2(\mathbf{L}, \mathbf{N}) < \frac{\varepsilon}{4}$. Such \mathbf{N} exists by classical Fourier analysis, see Pivato (2010, Theorem 9B.1). Let $\Upsilon := \max_{\mathbf{u} \in \mathcal{U}(\mathbf{L}, \mathbf{N})} \left| \widehat{f}(\mathbf{u}) - \vartheta(\mathbf{u}) \right|$. By the definition of $c_{\mathbf{k}}$ and $\tilde{c}_{\mathbf{k}}$, see Equation (3.11), it follows that

$$|c_{\mathbf{k}} - \tilde{c}_{\mathbf{k}}| \leq \frac{1}{2^{d-1} \prod_{h=1}^d L_h} \sum_{\mathbf{s} \in \mathcal{S}} \left| \widehat{f}\left(\frac{\pi}{2} \frac{\mathbf{s}\mathbf{k}}{\mathbf{L}}\right) - \vartheta\left(\frac{\pi}{2} \frac{\mathbf{s}\mathbf{k}}{\mathbf{L}}\right) \right| \leq \frac{\Upsilon}{\prod_{h=1}^d L_h}.$$

Similarly to the analysis of A_3 , we have

$$A_4(\mathbf{L}, \mathbf{N})^2 \leq \sum_{\mathbf{0} \leq \mathbf{k} \leq \mathbf{N}} \prod_{h=1}^d \{L_h\} |c_{\mathbf{k}} - \tilde{c}_{\mathbf{k}}|^2 \leq \frac{\Upsilon^2}{\prod_{h=1}^d L_h} \prod_{h=1}^d \{N_h + 1\}. \quad (3.19)$$

Choose $\delta = \frac{\varepsilon}{4} \sqrt{\prod_{h=1}^d L_h} \left(\prod_{h=1}^d \{N_h + 1\} \right)^{-\frac{1}{2}}$. Then $\Upsilon < \delta$ implies $A_4(\mathbf{L}, \mathbf{N}) < \frac{\varepsilon}{4}$, which concludes the proof. \square

The next two corollaries provide sufficient conditions to ensure that the classical COS-i and COS-iii methods and the damped COS-iv methods approximate the integral (3.6) within a predefined error tolerance $\varepsilon > 0$, including numerical uncertainty on \hat{f} .

Corollary 3.8. (Convergence of the classical COS-i and COS-iii methods). *Assume that Assumption A1 holds. The integral of the product of f and v can be approximated by a finite sum as follows: Let $\varepsilon > 0$. Let $\mathbf{M} \in \mathbb{R}_+^d$ and $\xi > 0$ such that*

$$\int_{\mathbb{R}^d \setminus [-\mathbf{M}, \mathbf{M}]} |v(\mathbf{x})f(\mathbf{x})| d\mathbf{x} \leq \frac{\varepsilon}{3}, \quad \|v1_{[-\mathbf{M}, \mathbf{M}]}\|_2 \leq \xi. \quad (3.20)$$

Let $\mathbf{L} \geq \mathbf{M}$ be such that

$$\|f - f1_{[-\mathbf{L}, \mathbf{L}]}\|_2 \leq \frac{\varepsilon}{12\xi} \quad (3.21)$$

and

$$B_f(\mathbf{L}) \leq \left(\frac{\varepsilon}{12\xi} \right)^2. \quad (3.22)$$

Choose $\mathbf{N} \in \mathbb{N}^d$ large enough, so that

$$\left\| f1_{[-\mathbf{L}, \mathbf{L}]} - \sum'_{\mathbf{0} \leq \mathbf{k} \leq \mathbf{N}} a_{\mathbf{k}} e_{\mathbf{k}} 1_{[-\mathbf{L}, \mathbf{L}]} \right\|_2 \leq \frac{\varepsilon}{12\xi}. \quad (3.23)$$

Let $c := \frac{\varepsilon}{12\xi} \frac{\sqrt{\prod_{h=1}^d L_h}}{\sqrt{\prod_{h=1}^d \{N_h + 1\}}}$. Then $c > 0$. For $\vartheta : \mathbb{R}^d \rightarrow \mathbb{C}$ assume

$$\max_{\mathbf{u} \in \mathcal{U}(\mathbf{L}, \mathbf{N})} |\hat{f}(\mathbf{u}) - \vartheta(\mathbf{u})| \leq c. \quad (3.24)$$

Then it follows that

$$\left| \int_{\mathbb{R}^d} v(\mathbf{x})f(\mathbf{x})d\mathbf{x} - \sum'_{\mathbf{0} \leq \mathbf{k} \leq \mathbf{N}} \tilde{c}_{\mathbf{k}} v_{\mathbf{k}} \right| \leq \varepsilon. \quad (3.25)$$

Corollary 3.9. (Convergence of the damped COS-iv method). *Assume that Assumption A2 holds. Let ε , ξ , \mathbf{L} , \mathbf{M} , \mathbf{N} , c and ϑ be as in Corollary 3.8. Let $\eta > 0$ such that $\sum'_{\mathbf{0} \leq \mathbf{k} \leq \mathbf{N}} |\tilde{c}_{\mathbf{k}}|^2 \leq \eta$. Assume that*

$$\sum'_{\mathbf{0} \leq \mathbf{k} \leq \mathbf{N}} |\tilde{v}_{\mathbf{k}} - v_{\mathbf{k}}|^2 \leq \frac{\varepsilon^2}{9\eta}. \quad (3.26)$$

Then it follows that $\left| \int_{\mathbb{R}^d} v(\mathbf{x})f(\mathbf{x})d\mathbf{x} - \sum'_{\mathbf{0} \leq \mathbf{k} \leq \mathbf{N}} \tilde{c}_{\mathbf{k}} \tilde{v}_{\mathbf{k}} \right| \leq \varepsilon$.

Proof. We first prove Corollary 3.9. Define $e_{\mathbf{k}}^{\mathbf{L}} = e_{\mathbf{k}}1_{[-\mathbf{L}, \mathbf{L}]}$. Let $A_1(\mathbf{L})$, $A_2(\mathbf{L}, \mathbf{N})$ and $A_4(\mathbf{L}, \mathbf{N})$ be as in the proof of Theorem 3.7. By Inequalities (3.19, 3.24) it follows that $A_4(\mathbf{L}, \mathbf{N}) \leq \frac{\varepsilon}{12\xi}$. Due to $v_{\mathbf{k}} = \langle v1_{[-M, M]}, e_{\mathbf{k}}^{\mathbf{L}} \rangle$ and applying Theorem 3.7 and the Cauchy-Schwarz inequality, we have that

$$\begin{aligned}
& \left| \int_{\mathbb{R}^d} v(\mathbf{x})f(\mathbf{x})d\mathbf{x} - \sum'_{\mathbf{0} \leq \mathbf{k} \leq \mathbf{N}} \tilde{c}_{\mathbf{k}}\tilde{v}_{\mathbf{k}} \right| \\
&= \left| \int_{\mathbb{R}^d \setminus [-M, M]} v(\mathbf{x})f(\mathbf{x})d\mathbf{x} + \langle v1_{[-M, M]}, f \rangle - \sum'_{\mathbf{0} \leq \mathbf{k} \leq \mathbf{N}} \tilde{c}_{\mathbf{k}}\langle v1_{[-M, M]}, e_{\mathbf{k}}^{\mathbf{L}} \rangle - \sum'_{\mathbf{0} \leq \mathbf{k} \leq \mathbf{N}} \tilde{c}_{\mathbf{k}}(\tilde{v}_{\mathbf{k}} - v_{\mathbf{k}}) \right| \\
&\leq \underbrace{\int_{\mathbb{R}^d \setminus [-M, M]} |v(\mathbf{x})f(\mathbf{x})|d\mathbf{x}}_{=:D_1(\mathbf{M})} + \left| \langle v1_{[-M, M]}, f - \sum'_{\mathbf{0} \leq \mathbf{k} \leq \mathbf{N}} \tilde{c}_{\mathbf{k}}e_{\mathbf{k}}^{\mathbf{L}} \rangle \right| + \underbrace{\sqrt{\left(\sum'_{\mathbf{0} \leq \mathbf{k} \leq \mathbf{N}} |\tilde{v}_{\mathbf{k}} - v_{\mathbf{k}}|^2 \right) \left(\sum'_{\mathbf{0} \leq \mathbf{k} \leq \mathbf{N}} |\tilde{c}_{\mathbf{k}}|^2 \right)}}_{=:D_2(\mathbf{N}, \mathbf{L}, \mathbf{M})} \\
&< \frac{\varepsilon}{3} + \|v1_{[-M, M]}\|_2 \left\| f - \sum'_{\mathbf{0} \leq \mathbf{k} \leq \mathbf{N}} \tilde{c}_{\mathbf{k}}e_{\mathbf{k}}^{\mathbf{L}} \right\|_2 + D_2(\mathbf{N}, \mathbf{L}, \mathbf{M}) \\
&< \frac{\varepsilon}{3} + \xi \left(A_1(\mathbf{L}) + A_2(\mathbf{L}, \mathbf{N}) + \sqrt{B_f(\mathbf{L})} + A_4(\mathbf{L}, \mathbf{N}) \right) + D_2(\mathbf{N}, \mathbf{L}, \mathbf{M}) \\
&\leq \frac{\varepsilon}{3} + \xi \left(\frac{\varepsilon}{12\xi} + \frac{\varepsilon}{12\xi} + \frac{\varepsilon}{12\xi} + \frac{\varepsilon}{12\xi} \right) + \frac{\varepsilon}{3} = \varepsilon.
\end{aligned}$$

To prove Corollary 3.8, replace $\tilde{v}_{\mathbf{k}}$ by $v_{\mathbf{k}}$ in the inequalities above. Then, $D_2(\mathbf{N}, \mathbf{L}, \mathbf{M}) = 0$, and the assertion in Corollary 3.8 will follow. \square

Remark 3.10. From the proof of Corollary 3.8, it can be seen that the Inequalities (3.20 - 3.24) could be strengthened replacing $\frac{\varepsilon}{3}$ with $\frac{\varepsilon}{2}$ and $\frac{\varepsilon}{12\xi}$ with $\frac{\varepsilon}{8\xi}$. The convergence of the classical COS-ii method approximating $v_{\mathbf{k}}$ numerically by $v_{\mathbf{k}}^{\text{Num}}$ follows as in Corollary 3.9 replacing $\tilde{v}_{\mathbf{k}}$ by $v_{\mathbf{k}}^{\text{Num}}$.

Remark 3.11. Sufficient conditions such that Inequality (3.26) holds are provided in Corollary 3.16.

Remark 3.12. We do not need all conditions in Assumption A1 to prove Theorem 3.7 and Corollary 3.8: f does not need to decay exponentially and v does not need to be bounded; it is sufficient that v is locally in $\mathcal{L}^1 \cap \mathcal{L}^2$.

Remark 3.13. Inequality (3.24) tells us how close the approximation ϑ has to be to \hat{f} to ensure that the overall error of the COS-i, COS-iii or COS-iv method is utmost ε . In Section 6.1, we approximate \hat{f} by numerically solving an ODE, and Inequality (3.24) helps us to choose the number of steps for the Euler method.

Remark 3.14. \mathbf{M} and \mathbf{L} in the Corollaries 3.8 and 3.9 play different roles: \mathbf{M} depends mainly on v and \mathbf{L} depends only on f . For example, if v is bounded by a very small bound, the conditions in (3.20) are satisfied for \mathbf{M} close to zero. However, to satisfy Inequalities (3.21, 3.22), it might be necessary to choose \mathbf{L} much larger than \mathbf{M} .

The next theorem and two corollaries provide an explicit formula for the truncation range and an implicit formula for the number of terms for the classical COS-i and COS-iii methods and the damped COS-iv method.

Theorem 3.15. (Classical COS-i and COS-iii methods: Find \mathbf{M} and \mathbf{L}). *Assume that Assumption A1 holds. Let $n \geq 2$ be an even number and assume that the moments of f of n^{th} -order exist, i.e.,*

$$m_h(n) := \int_{\mathbb{R}^d} x_h^n f(\mathbf{x})d\mathbf{x} = i^{-n} \frac{\partial^n}{\partial u_h^n} \hat{f}(\mathbf{u}) \Big|_{\mathbf{u}=\mathbf{0}} \in (0, \infty), \quad h = 1, \dots, d. \quad (3.27)$$

Let $\varepsilon > 0$ be small enough. Define

$$M_h := \left(\frac{3d \|v\|_{\infty} m_h(n)}{\varepsilon} \right)^{\frac{1}{n}}, \quad h = 1, \dots, d, \quad (3.28)$$

and $\mathbf{L} = \mathbf{M} = (M_1, \dots, M_d) \in \mathbb{R}_+^d$. There is a $\mathbf{N} \in \mathbb{N}_0^d$ such that

$$\left| \int_{\mathbb{R}^d} v(\mathbf{x})f(\mathbf{x})d\mathbf{x} - \sum'_{\mathbf{0} \leq \mathbf{k} \leq \mathbf{N}} c_{\mathbf{k}}v_{\mathbf{k}} \right| \leq \varepsilon. \quad (3.29)$$

Corollary 3.16. (Damped COS-iv method: Find \mathbf{M} and \mathbf{L}). *Let \mathbf{M} and \mathbf{L} be as in Theorem 3.15. Assume that Assumption A2 holds. There is a $\mathbf{N} \in \mathbb{N}_0^d$ such that*

$$\left| \int_{\mathbb{R}^d} v(\mathbf{x})f(\mathbf{x})d\mathbf{x} - \sum'_{\mathbf{0} \leq \mathbf{k} \leq \mathbf{N}} c_{\mathbf{k}}\tilde{v}_{\mathbf{k}} \right| \leq \varepsilon. \quad (3.30)$$

Corollary 3.17. (Classical COS-i, COS-iii and damped COS-iv methods: Find \mathbf{N}). *Let \mathbf{M} and \mathbf{L} be as in Theorem 3.15. Let $\xi > 0$ such that $\|v1_{[-\mathbf{M}, \mathbf{M}]} \|_2 \leq \xi$. Suppose for some $\mathbf{N} \in \mathbb{N}_0^d$ it holds that*

$$\left| (2\pi)^{-d} \int_{\mathbb{R}^d} |\widehat{f}(\mathbf{u})|^2 d\mathbf{u} - \prod_{h=1}^d L_h \sum'_{\mathbf{0} \leq \mathbf{k} \leq \mathbf{N}} |c_{\mathbf{k}}|^2 \right| \leq \frac{\varepsilon^2}{162\xi^2}. \quad (3.31)$$

If Assumption A1 is satisfied then Inequality (3.29) holds and if Assumption A2 is satisfied then Inequality (3.30) holds.

Proof. We first prove Theorem 3.15: Assumption A1 implies that $f \geq 0$, f decays exponentially and v is bounded. Equation (3.27) follows by Bauer (1996, Thm 25.2). For $h \in \{1, \dots, d\}$ let $\pi_h : \mathbb{R}^d \rightarrow \mathbb{R}$, $\mathbf{x} \mapsto x_h$. Let $\lambda_{\text{Lebesgue}}^d$ be the Lebesgue measure on \mathbb{R}^d and define the finite and positive measure $\zeta := f\lambda_{\text{Lebesgue}}^d$. By Markov's inequality, it follows that

$$\int_{\mathbb{R}^d \setminus [-\mathbf{M}, \mathbf{M}]} |v(\mathbf{x})f(\mathbf{x})| d\mathbf{x} \leq \|v\|_{\infty} \sum_{h=1}^d \zeta(\{\mathbf{x} \in \mathbb{R}^d : |\pi_h(\mathbf{x})| \geq M_h\}) \leq \|v\|_{\infty} \sum_{h=1}^d \frac{m_h(n)}{M_h^n} = \frac{\varepsilon}{3}.$$

The last equality follows by the definition of \mathbf{M} . Define $\xi := \|v\|_{\infty} \sqrt{2^d \prod_{h=1}^d M_h}$. It holds that $\|v1_{[-\mathbf{M}, \mathbf{M}]} \|_2 \leq \xi$. Hence, the inequalities in (3.20) are satisfied. Next, we use the following auxiliary result: Let $s \geq 0$, $a > 0$ and $n \in \mathbb{N}_0$ and $d \in \mathbb{N}$. Then it holds by mathematical induction over n and Amann and Escher (2009, Theorem 8.11) that

$$\int_{\{\mathbf{x} \in \mathbb{R}^d : |\mathbf{x}| > s\}} e^{-a|\mathbf{x}|} |\mathbf{x}|^n d\mathbf{x} = \frac{d\pi^{\frac{d}{2}}}{\Gamma(1 + \frac{d}{2})} e^{-as} \frac{(n+d-1)!}{a^{n+d}} \sum_{k=0}^{n+d-1} \frac{(as)^k}{k!}. \quad (3.32)$$

For ε small enough, \mathbf{L} is large enough. Using that f decays exponentially and applying Equation (3.32), we obtain with $\ell := \min_{h=1, \dots, d} L_h$ that

$$\|f - f1_{[-\mathbf{L}, \mathbf{L}]} \|_2 \leq C_1 \sqrt{\int_{\{\mathbf{x} \in \mathbb{R}^d : |\mathbf{x}| > \ell\}} e^{-2C_2|\mathbf{x}|} d\mathbf{x}} \leq \frac{\varepsilon}{12\xi}. \quad (3.33)$$

The last inequality holds true if ε is small enough because, thanks to Equality (3.32), the term in the middle of (3.33) decreases exponentially in ε , while the term at the right-hand side of (3.33) goes to zero like $\varepsilon^{1 + \frac{d}{2n}}$ for $\varepsilon \searrow 0$. Hence, Inequality (3.21) holds. By Inequality (A.2) it holds that $B_f(\mathbf{L}) \leq \varepsilon^2(12\xi)^{-2}$ if ε is small enough because $B_f(\mathbf{L})$ decreases exponentially in ε : to see this, use Inequality (3.33) and observe that the term $\int_{\mathbb{R}^d \setminus [-\mathbf{L}, \mathbf{L}]} |\mathbf{x}|^{2d} |f(\mathbf{x})|^2 d\mathbf{x}$ converges exponentially thanks to Inequality (3.32). Hence, Inequality (3.22) holds. By classical Fourier analysis, there is a $\mathbf{N} \in \mathbb{N}_0^d$ such that Inequality (3.23) is satisfied. By assumption we have $c_{\mathbf{k}} = \tilde{c}_{\mathbf{k}}$. Inequality (3.24) holds trivially. Apply Corollary 3.8 to finish the proof of Theorem 3.15.

We prove Corollary 3.16: We have to show that Inequality (3.26) holds to prove Corollary 3.16. Let $G(\mathbf{L})$ be as in Equality (A.7). Observe $G(\mathbf{L}) \rightarrow 0$, $\min_h L_h \rightarrow \infty$ because f is COS-admissible by Proposition

A.1. There is $\mathbf{P} \in \mathbb{R}_+^d$ and a $\delta > 0$ such that $G(\mathbf{L}) \leq \delta$ for all $\mathbf{L} \geq \mathbf{P}$. By Inequality (A.9), it follows for all $\mathbf{N} \in \mathbb{N}^d$ and all $\mathbf{L} \geq \mathbf{P}$ that

$$\sum'_{\mathbf{0} \leq \mathbf{k} \leq \mathbf{N}} |c_{\mathbf{k}}|^2 \leq \frac{\int_{\mathbb{R}^d} |f(\mathbf{x})|^2 d\mathbf{x} + \delta}{\prod_{h=1}^d P_h} =: \eta < \infty. \quad (3.34)$$

It follows by Proposition A.1 for all $\mathbf{N} \in \mathbb{N}^d$ that

$$\sum'_{\mathbf{0} \leq \mathbf{k} \leq \mathbf{N}} |\tilde{v}_{\mathbf{k}} - v_{\mathbf{k}}|^2 \leq \sum'_{\mathbf{k} \in \mathbb{N}_0^d} \left| \int_{\mathbb{R}^d \setminus [-M, M]} v(\mathbf{x}) e_{\mathbf{k}}(\mathbf{x}) d\mathbf{x} \right|^2 \leq \prod_{h=1}^d M_h B_v(\mathbf{M}) \leq \frac{\varepsilon^2}{9\eta} \quad (3.35)$$

the last inequality holds true if ε is small enough because the term $M_h B_v(\mathbf{M})$ decreases exponentially in ε since v decays exponentially, while the right-hand side of (3.35) goes to zero like ε^2 for $\varepsilon \searrow 0$.

We prove Corollary 3.17: Let $G(\mathbf{L})$ be defined as in Equation (A.7). By Lemma A.3 and the Plancherel theorem, it follows that

$$\begin{aligned} \|f1_{[-L, L]} - \sum'_{\mathbf{0} \leq \mathbf{k} \leq \mathbf{N}} a_{\mathbf{k}} e_{\mathbf{k}} 1_{[-L, L]}\|_2^2 &\leq \left| (2\pi)^{-d} \int_{\mathbb{R}^d} |\widehat{f}(\mathbf{u})|^2 d\mathbf{u} - \prod_{h=1}^d L_h \sum'_{\mathbf{0} \leq \mathbf{k} \leq \mathbf{N}} |c_{\mathbf{k}}|^2 \right| + G(\mathbf{L}) \\ &\leq \frac{\varepsilon^2}{162 \|v1_{[-M, M]}\|_2^2} + \frac{\varepsilon^2}{162 \|v1_{[-M, M]}\|_2^2} = \left(\frac{\varepsilon}{9 \|v1_{[-M, M]}\|_2} \right)^2. \end{aligned} \quad (3.36)$$

The last inequality holds because for $\varepsilon > 0$ small enough, \mathbf{L} is large enough so that $G(\mathbf{L}) \leq \frac{\varepsilon^2}{162 \|v1_{[-M, M]}\|_2^2}$ since $G(\mathbf{L})$ decreases exponentially. Note that we may replace the term $\frac{\varepsilon}{12\varepsilon}$ in Inequalities (3.21, 3.22, 3.23) in Corollary 3.8 by $\frac{\varepsilon}{9 \|v1_{[-M, M]}\|_2}$, since $c_{\mathbf{k}} = \tilde{c}_{\mathbf{k}}$. Apply Inequality (3.36) to conclude. \square

Assume the density f in Corollary 3.17 is the density of a Lévy process at a particular time point and \widehat{f} is real. The next Proposition 3.18 shows that the term $(2\pi)^{-d} \int_{\mathbb{R}^d} |\widehat{f}(\mathbf{u})|^2 d\mathbf{u}$ is then given in closed form if f is known. The densities of many Lévy processes are given explicitly or in terms of specialized functions, e.g., for the Meixner process, the Normal Inverse Gaussian process, the Variance Gamma process and the Generalized Hyperbolic process, see Barndorff-Nielsen (1997); Madan et al. (1998); Schoutens (2003) and references therein. For example, the multivariate Brownian motion at time $T > 0$ has a multivariate normal density and the corresponding Fourier transform is real (with or without damping), see Example 4.1.

Proposition 3.18. *Let $(\mathbf{X}_t)_{t \geq 0}$ be a d -dimensional Lévy process. Assume that the characteristic function $\widehat{f}_{\mathbf{X}_t}$ of \mathbf{X}_t is real for all $t > 0$ and that \mathbf{X}_t has a density, denoted by $f_{\mathbf{X}_t}$. Let $T > 0$. Then*

$$(2\pi)^{-d} \int_{\mathbb{R}^d} |\widehat{f}_{\mathbf{X}_T}(\mathbf{u})|^2 d\mathbf{u} = f_{\mathbf{X}_{2T}}(\mathbf{0}).$$

Proof. Using that \mathbf{X} has independent and stationary increments and that $\widehat{f}_{\mathbf{X}_T}$ is real, it follows that

$$(2\pi)^{-d} \int_{\mathbb{R}^d} |\widehat{f}_{\mathbf{X}_T}(\mathbf{u})|^2 d\mathbf{u} = (2\pi)^{-d} \int_{\mathbb{R}^d} (\widehat{f}_{\mathbf{X}_T}(\mathbf{u}))^2 d\mathbf{u} = (2\pi)^{-d} \int_{\mathbb{R}^d} \widehat{f}_{\mathbf{X}_{2T}}(\mathbf{u}) d\mathbf{u} = f_{\mathbf{X}_{2T}}(\mathbf{0}).$$

\square

Remark 3.19. Provided the expression $(2\pi)^{-d} \int_{\mathbb{R}^d} |\widehat{f}(\mathbf{u})|^2 d\mathbf{u}$ can be obtained precisely, Inequality (3.31) makes it possible to define a stopping criterion for \mathbf{N} . In particular, Inequality (3.31) enables us to determine \mathbf{N} while computing the coefficients $c_{\mathbf{k}}$: incrementally increase \mathbf{N} and compute $c_{\mathbf{k}}$ and $|c_{\mathbf{k}}|^2$ simultaneously. Stop when Inequality (3.31) is met. This is explained in more detail in Algorithm 2. However, since the right-hand side of Equation (3.31) converges to zero at least like $O(\varepsilon^2)$, rounding off errors makes it difficult to find \mathbf{N} by Inequality (3.31) for very small ε . Using arbitrary-precision arithmetic instead of fixed-precision arithmetic should overcome this drawback.

The next theorem implies that classical COS-i and COS-iii and the damped COS-iv methods converge exponentially if \widehat{f} decays exponentially, i.e., if Inequality (3.37) holds for all $p > 0$. The Cases (a) and (b) in Theorem 3.20 treat the classical COS-i and COS-ii methods and the damped COS-iv method, respectively. The bound for the order of convergence of the damped COS-iv method is slightly better.

Theorem 3.20. (*Order of convergence*). Let $\gamma > 0$ and $\beta \in (0, 1)$. For $n \in \mathbb{N}$, let $\mathbf{N} = (n, \dots, n) \in \mathbb{N}^d$ and $\mathbf{M} = \mathbf{L} = (\gamma n^\beta, \dots, \gamma n^\beta)$. Assume for some $p > \frac{d}{2}$ that

$$|\widehat{f}(\mathbf{u})| \leq O(|\mathbf{u}|_\infty^{-p}), \quad |\mathbf{u}|_\infty \rightarrow \infty. \quad (3.37)$$

(a) (Classical COS-i or COS-iii methods). Assume that Assumption A1 holds. Then it follows that

$$\left| \int_{\mathbb{R}^d} v(\mathbf{x})f(\mathbf{x})d\mathbf{x} - \sum'_{\mathbf{0} \leq \mathbf{k} \leq \mathbf{N}} c_{\mathbf{k}}v_{\mathbf{k}} \right| \leq O\left(n^{-(1-\beta)p+\frac{d}{2}}\right), \quad n \rightarrow \infty.$$

(b) (Damped COS-iv method). Assume that Assumptions A2 holds. Then it follows that

$$\left| \int_{\mathbb{R}^d} v(\mathbf{x})f(\mathbf{x})d\mathbf{x} - \sum'_{\mathbf{0} \leq \mathbf{k} \leq \mathbf{N}} c_{\mathbf{k}}\tilde{v}_{\mathbf{k}} \right| \leq O\left(n^{-(1-\beta)(p-\frac{d}{2})}\right), \quad n \rightarrow \infty.$$

Proof. Let $A_1(\mathbf{L})$, $A_2(\mathbf{L}, \mathbf{N})$, $D_1(\mathbf{M})$ and $D_2(\mathbf{N}, \mathbf{L}, \mathbf{M})$ be as in the proof of Corollary 3.8. Since $v_{\mathbf{k}} = \langle v1_{[-\mathbf{M}, \mathbf{M}]}, e_{\mathbf{k}}^{\mathbf{L}} \rangle$ and similarly to the proof of Corollary 3.8 we have that

$$\begin{aligned} & \left| \int_{\mathbb{R}^d} v(\mathbf{x})f(\mathbf{x})d\mathbf{x} - \sum'_{\mathbf{0} \leq \mathbf{k} \leq \mathbf{N}} c_{\mathbf{k}}r_{\mathbf{k}} \right| \\ & \leq D_1(\mathbf{M}) + \|v1_{[-\mathbf{M}, \mathbf{M}]\|_2 \left(A_1(\mathbf{L}) + A_2(\mathbf{L}, \mathbf{N}) + \sqrt{B_f(\mathbf{L})} \right) + D_2(\mathbf{N}, \mathbf{L}, \mathbf{M}), \end{aligned} \quad (3.38)$$

where $r_{\mathbf{k}} := v_{\mathbf{k}}$ in case a) and $r_{\mathbf{k}} := \tilde{v}_{\mathbf{k}}$ in case b). We will analyze the order of convergence of each term at the right-hand side of Inequality (3.38): Since v is bounded and f decays exponentially, $D_1(\mathbf{M})$, $A_1(\mathbf{L})$ and $\sqrt{B_f(\mathbf{L})}$ decay exponentially, i.e., can be bounded by $O(\exp(-C_3n^\beta))$, $n \rightarrow \infty$, for some C_3 , see proof of Theorem 3.15. By Inequality (3.34), the term $\sum' |c_{\mathbf{k}}|^2$ is bounded. In case a), $D_2(\mathbf{N}, \mathbf{L}, \mathbf{M}) = 0$. In case b), $D_2(\mathbf{N}, \mathbf{L}, \mathbf{M})$ decays exponentially, see proof of Corollary 3.16. Last, we treat $A_2(\mathbf{L}, \mathbf{N})$. Let $j \in \{1, \dots, d\}$. Let n be large enough. Let $\mathbf{k} \in \mathbb{N}_0^d$ such that $k_j > n$. By Equation (3.11), Inequality (3.37) and using $L_h = \gamma n^\beta$, $h = 1, \dots, d$, there is a constant $a_1 > 0$ so that

$$|c_{\mathbf{k}}|^2 \stackrel{(3.11)}{\leq} \left(\frac{1}{2^{d-1} \prod_{h=1}^d L_h} \sum_{\mathbf{s} \in \mathcal{S}} \left| \widehat{f}\left(\frac{\pi \mathbf{s} \mathbf{k}}{2 \mathbf{L}}\right) \right| \right)^2 \stackrel{(3.37)}{\leq} a_1 \left(\frac{1}{n^{d\beta}} \left(\frac{|\mathbf{k}|_\infty}{n^\beta} \right)^{-p} \right)^2 = a_1 n^{2\beta(p-d)} |\mathbf{k}|_\infty^{-2p}.$$

By mathematical induction over d and the applying the integral test of convergence, one can show that

$$\sum_{\mathbf{k} \in \mathbb{N}_0^d, k_j > n} |\mathbf{k}|_\infty^{-2p} \leq \frac{2^{d-1}}{(2p-d)n^{2p-d}}. \quad (3.39)$$

It follows by Inequality (3.39) for some $a_2 > 0$ that

$$\prod_{h=1}^d L_h \sum_{\mathbf{k} \in \mathbb{N}_0^d, k_j > n} |c_{\mathbf{k}}|^2 \leq a_2 n^{-(1-\beta)(2p-d)}. \quad (3.40)$$

Let $G(\mathbf{L})$ be defined as in Equality (A.7). By Equality (3.18), the Cauchy-Schwarz (CS) inequality and Inequality (A.9), we obtain

$$\begin{aligned}
A_2(\mathbf{L}, N)^2 &\stackrel{(3.18)}{\leq} \prod_{h=1}^d L_h \sum'_{k_1 > N_1 \text{ or } \dots \text{ or } k_d > N_d} |a_{\mathbf{k}} + c_{\mathbf{k}} - c_{\mathbf{k}}|^2 \\
&\stackrel{(CS)}{\leq} \prod_{h=1}^d L_h \sum'_{k_1 > N_1 \text{ or } \dots \text{ or } k_d > N_d} |c_{\mathbf{k}}|^2 + \prod_{h=1}^d L_h \sum'_{\mathbf{k} \in \mathbb{N}_0^d} |a_{\mathbf{k}} - c_{\mathbf{k}}|^2 \\
&\quad + 2 \sqrt{\prod_{h=1}^d L_h \sum'_{\mathbf{k} \in \mathbb{N}_0^d} |c_{\mathbf{k}}|^2 \prod_{h=1}^d L_h \sum'_{\mathbf{k} \in \mathbb{N}_0^d} |a_{\mathbf{k}} - c_{\mathbf{k}}|^2} \\
&\stackrel{(A.9)}{\leq} \sum_{j=1}^d \left(\prod_{h=1}^d L_h \sum_{\mathbf{k} \in \mathbb{N}_0^d, k_j > n} |c_{\mathbf{k}}|^2 \right) + B_f(\mathbf{L}) + 2 \sqrt{\left(\int_{\mathbb{R}^d} |f(\mathbf{x})|^2 d\mathbf{x} + G(\mathbf{L}) \right) B_f(\mathbf{L})} \\
&\stackrel{(3.40)}{\leq} O\left(n^{-(1-\beta)(2p-d)}\right), \quad n \rightarrow \infty,
\end{aligned}$$

since $B_f(\mathbf{L})$ and $G(\mathbf{L})$, converge exponentially to zero. Since v is bounded, we have that $\|v1_{[-M, M]}\|_2 \leq O\left(n^{\frac{d\beta}{2}}\right)$, $n \rightarrow \infty$. Noting that $\frac{-(1-\beta)(2p-d)+d\beta}{2} = -(1-\beta)p + \frac{d}{2}$, shows (a). It holds $\|v1_{[-M, M]}\|_2 \leq \|v\|_2$ if $v \in \mathcal{L}^2$, which implies (b). \square

4 Characteristic functions

In this section, in Examples 4.1 and 4.2, we recall the multivariate normal and the Variance Gamma distributions from the literature. Remark 4.4 and Examples 4.5 and 4.6 provide a financial context.

Example 4.1. (Multivariate normal distribution). Let \mathbf{X} be a multivariate normal random variable with location $\boldsymbol{\eta} \in \mathbb{R}^d$ and covariance matrix $\Sigma \in \mathbb{R}^{d \times d}$. The random variable \mathbf{X} has characteristic function $\widehat{g}(\mathbf{u}) = \exp(i\boldsymbol{\eta} \cdot \mathbf{u} - \frac{1}{2}\mathbf{u} \cdot \Sigma \mathbf{u})$, $\mathbf{u} \in \mathbb{R}^d$, which can be extended to \mathbb{C}^d , i.e., $\widehat{g}(\mathbf{u} - i\boldsymbol{\alpha})$ exists for all $\boldsymbol{\alpha} \in \mathbb{R}^d$ and for the set δ_g , defined in Equation (3.1), it holds that $\delta_g = \mathbb{R}^d$. By Proposition A.2 we set $\lambda = \exp(-\boldsymbol{\eta} \cdot \boldsymbol{\alpha} - \frac{1}{2}\boldsymbol{\alpha} \cdot \Sigma \boldsymbol{\alpha})$ and $\boldsymbol{\mu} = \boldsymbol{\eta} + \Sigma \boldsymbol{\alpha}$. The characteristic function of the damped density f , defined in Equation (3.4), is given by $\widehat{f}(\mathbf{u}) = \exp(-\frac{1}{2}\mathbf{u} \cdot \Sigma \mathbf{u})$, which is the characteristic function of a multivariate normal random variable with location zero and covariance matrix Σ . A straightforward computation shows that

$$(2\pi)^{-d} \int_{\mathbb{R}^d} |\widehat{f}(\mathbf{u})|^2 d\mathbf{u} = \frac{2^{-d}}{\sqrt{\pi^d \det(\Sigma)}}.$$

Example 4.2. (Variance Gamma distribution). Let \mathbf{Z} be a d -dimensional, standard normal random variable. Let G be a Gamma distributed random variable, independent of \mathbf{Z} , with shape $a > 0$ and scale $s > 0$. Let $\boldsymbol{\eta}, \boldsymbol{\theta} \in \mathbb{R}^d$ and $\boldsymbol{\sigma} \in \mathbb{R}_+^d$. Consider $\mathbf{X} = \boldsymbol{\eta} + \boldsymbol{\theta}G + \sqrt{G}\boldsymbol{\sigma}\mathbf{Z}$. The distribution of \mathbf{X} is denoted by $\text{VG}(a, s, \boldsymbol{\eta}, \boldsymbol{\theta}, \boldsymbol{\sigma})$. Throughout the paper we assume that $a > \frac{1}{2}$. Define $\Sigma \in \mathbb{R}^{d \times d}$ such that $\Sigma_{ii} = \sigma_i^2$ and $\Sigma_{ij} = 0$ for $i \neq j$. Then \mathbf{X} has the characteristic function

$$\widehat{g}(\mathbf{u}) = \exp(i\boldsymbol{\eta} \cdot \mathbf{u}) \left(1 - is\boldsymbol{\theta} \cdot \mathbf{u} + \frac{1}{2}s\mathbf{u} \cdot \Sigma \mathbf{u}\right)^{-a},$$

see Luciano and Schoutens (2006). These authors propose the simplifying assumption that Σ is a diagonal matrix to ensure that the number of parameters of the VG distribution increases linearly with the dimension d . The (extended) Fourier transform $\widehat{g}(\mathbf{u} - i\boldsymbol{\alpha})$ exists for all $\boldsymbol{\alpha} \in \mathbb{R}^d$ with $\zeta(\boldsymbol{\alpha}) := 1 - s\boldsymbol{\theta} \cdot \boldsymbol{\alpha} - \frac{1}{2}s\boldsymbol{\alpha} \cdot \Sigma \boldsymbol{\alpha} > 0$, see Bayer et al. (2023). By Proposition A.2, we set $\lambda = \exp(-\boldsymbol{\eta} \cdot \boldsymbol{\alpha}) (\zeta(\boldsymbol{\alpha}))^a$ and $\boldsymbol{\mu} = \boldsymbol{\eta} + as\zeta^{-1}(\boldsymbol{\theta} + \Sigma \boldsymbol{\alpha})$. The characteristic function of the damped density f , defined in Equation (3.4), is given by

$$\widehat{f}(\mathbf{u}) = \exp\left(-i\frac{as}{\zeta(\boldsymbol{\alpha})}(\boldsymbol{\theta} + \Sigma \boldsymbol{\alpha}) \cdot \mathbf{u}\right) \left(1 - i\frac{s}{\zeta(\boldsymbol{\alpha})}(\boldsymbol{\theta} + \Sigma \boldsymbol{\alpha}) \cdot \mathbf{u} + \frac{1}{2}\frac{s}{\zeta(\boldsymbol{\alpha})}\mathbf{u} \cdot \Sigma \mathbf{u}\right)^{-a},$$

which is the characteristic function of a VG $\left(a, \frac{s}{\zeta(\boldsymbol{\alpha})}, -\frac{as}{\zeta(\boldsymbol{\alpha})}(\boldsymbol{\theta} + \Sigma\boldsymbol{\alpha}), \boldsymbol{\theta} + \Sigma\boldsymbol{\alpha}, \boldsymbol{\sigma}\right)$ distributed random variable. Using the fact that Σ is a diagonal matrix, it holds for $|\mathbf{u}|_\infty$ large enough that

$$|\widehat{f}(\mathbf{u})|^2 \leq \left(\frac{1}{2} \frac{s}{\zeta(\boldsymbol{\alpha})} \mathbf{u} \cdot \Sigma \mathbf{u}\right)^{-2a} \leq (c_1 |\mathbf{u}|^2)^{-2a} \leq c_2 |\mathbf{u}|_\infty^{-4a}$$

for suitable constants $c_1, c_2 > 0$. Since \widehat{f} is bounded by 1, this implies that $|\widehat{f}(\mathbf{u})| \leq O(|\mathbf{u}|_\infty^{-2a})$ for $|\mathbf{u}|_\infty \rightarrow \infty$. Since $a > \frac{1}{2}$, \widehat{f} is integrable, which implies that f is continuous and bounded. In particular, $f \in \mathcal{L}^1 \cap \mathcal{L}^2$. Since the marginal densities of f are VG distributed and have semi-heavy tails, see Küchler and Tappe (2008), f decays exponentially if $\zeta(\boldsymbol{\alpha}) > 0$. For the set δ_g , defined in Equation (3.1), it holds that $\delta_g = \{\boldsymbol{\alpha} \in \mathbb{R}^d : \zeta(\boldsymbol{\alpha}) > 0\}$. Note that $\mathbf{0} \in \delta_g$ and δ_g is open.

Remark 4.3. The Assumption that \widehat{f} is integrable in Example 4.2, i.e., $a > \frac{1}{2}$, is also made in Eberlein et al. (2010, Remark 2.3 and Assumption A3) to treat discontinuous functions of interest, e.g., to obtain a CDF.

Remark 4.4. In a financial context, we model d stock prices over time by a d -dimensional positive semimartingale $(\mathbf{S}(t))_{t \geq 0}$ on a filtered probability space $(\Omega, \mathcal{F}, P, (\mathcal{F}_t)_{t \geq 0})$. The filtration $(\mathcal{F}_t)_{t \geq 0}$ satisfies the usual conditions with $\mathcal{F}_0 = \{\Omega, \emptyset\}$. The logarithmic returns are defined by $\mathbf{X}(t) := \log(\mathbf{S}(t))$, $t \geq 0$. There is a bank account paying continuous compound interest $r \in \mathbb{R}$. There is a European option $w : \mathbb{R}^d \rightarrow \mathbb{R}$ with maturity $T > 0$ and payoff $w(\mathbf{X}(T))$ at time T . We denote by g the (risk-neutral) density of $\log(\mathbf{S}(T))$. The time-0 price of the European option is then given by $e^{-rT} \int_{\mathbb{R}^d} w(\mathbf{x})g(\mathbf{x})d\mathbf{x}$. This integral can be approximated by the classical COS-i, COS-ii, COS-iii or the damped COS-iv method.

Example 4.5. (BS model). Let $\Sigma \in \mathbb{R}^{d \times d}$ be a symmetric positive definite matrix. For the Black-Scholes (BS) model, the logarithmic returns $\mathbf{X}(T)$ are normally distributed with location $\boldsymbol{\eta} := \log(\mathbf{S}(0)) + (\mathbf{r} - \frac{1}{2}\text{diag}(\Sigma))T$ and covariance matrix $T\Sigma$, where $\mathbf{r} = (r, \dots, r) \in \mathbb{R}^d$ and $\text{diag}(\Sigma) \in \mathbb{R}^d$ denotes the diagonal of Σ .

Example 4.6. (VG model). Let $\nu > 0$, $\boldsymbol{\sigma} \in \mathbb{R}_+^d$ and $\boldsymbol{\theta} \in \mathbb{R}^d$. In the multivariate Variance Gamma (VG) model, see Luciano and Schoutens (2006), the logarithmic returns $\mathbf{X}(T)$ follow a $\text{VG}(\frac{T}{\nu}, \nu, \boldsymbol{\eta}, \boldsymbol{\theta}, \boldsymbol{\sigma})$ distribution, where

$$\eta_h := \log(S_h(0)) + \left(r + \frac{1}{\nu} \log\left(1 - \frac{1}{2}\sigma_h^2\nu - \theta_h\nu\right)\right)T, \quad h = 1, \dots, d.$$

As in Example 4.2, we assume $\frac{T}{\nu} > \frac{1}{2}$ to ensure that the density of the VG distribution is square-integrable. Carr and Madan (1999) calibrated the one-dimensional VG model to real market data and observed an average value of $\nu = 0.16$. Luciano and Schoutens (2006) calibrated a three-dimensional VG model with stochastic time change to real market data and obtained a similar value for ν . For such ν , only options with a maturity greater than about one month satisfy the condition $\frac{T}{\nu} > \frac{1}{2}$, which limits the applicability of the COS method in the VG model for options with short maturities.

5 Functions of interest

Example 5.1. (CDF by the classical COS-i method). Let $w(\mathbf{x}) = 1_{(-\infty, \mathbf{y}]}$, $\mathbf{x} \in \mathbb{R}^d$ for some $\mathbf{y} \in \mathbb{R}^d$. Then $v(\mathbf{x}) = 1_{(-\infty, \mathbf{y}]}(\mathbf{x} + \boldsymbol{\mu})$ for shift parameter $\boldsymbol{\mu}$. Since w is bounded and zero outside $(-\infty, \mathbf{y}]$, it holds that $\delta_w^\infty = \mathbb{R}_+^d$, where δ_w^∞ is defined in Equation (3.2). The integral in (1.1) is equal to the CDF of the density g evaluated at \mathbf{y} . The coefficients $v_{\mathbf{k}}$, defined in Equation (3.14), can be obtained in closed form: Let $\mathbf{M}, \mathbf{L} \in \mathbb{R}_+^d$ as in Section 3. It holds for $\mathbf{k} \in \mathbb{N}_0^d$ that $v_{\mathbf{k}} = 0$ if $y_h - \mu_h < -M_h$ for any h , and otherwise

$$\begin{aligned} v_{\mathbf{k}} &= \prod_{h=1}^d \int_{-M_h}^{M_h} 1_{(-\infty, y_h]}(x + \mu_h) \cos\left(k_h \pi \frac{x + L_h}{2L_h}\right) dx \\ &= \prod_{\substack{h=1 \\ k_h=0}}^d \{A_h + M_h\} \prod_{\substack{h=1 \\ k_h>0}}^d \left\{ \frac{2L_h}{\pi k_h} \left(\sin\left(k_h \pi \frac{A_h + L_h}{2L_h}\right) - \sin\left(k_h \pi \frac{-M_h + L_h}{2L_h}\right) \right) \right\}, \end{aligned} \quad (5.1)$$

where $A_h := \min(y_h - \mu_h, M_h)$. It holds that $\|v\|_\infty \leq 1$ and $\|v1_{[-M, M]}\|_2^2 \leq 2^d \prod_{h=1}^d M_h$.

We also discuss the possibility of approximating the CDF by the damped COS-iv method in Example 5.2 to test the damped COS-iv and to be able to compare the damped and the classical COS-i methods. In real world applications we recommend applying Example 5.1 instead of Example 5.2 to approximate a CDF since the classical COS-i method does not require a damping factor and can therefore be applied more straightforwardly.

Example 5.2. (CDF by the damped COS-iv method). Let w be as in Example 5.1. A simple calculation shows that the Fourier transform of w exists for $\mathbf{z} \in \mathbb{C}^d$ such that $\Im\{z_h\} < 0$, $h = 1, \dots, d$, and is given by $\widehat{w}(\mathbf{z}) = \prod_{h=1}^d \frac{e^{iy_h z_h}}{iz_h}$. Hence, for $\boldsymbol{\alpha} < \mathbf{0}$, it holds that

$$\int_{\mathbb{R}^d} |w(\mathbf{x})e^{-\boldsymbol{\alpha} \cdot \mathbf{x}}| d\mathbf{x} = \int_{\mathbb{R}^d} w(\mathbf{x})e^{-\boldsymbol{\alpha} \cdot \mathbf{x}} d\mathbf{x} = \widehat{w}(i\boldsymbol{\alpha}) \in \mathbb{R}.$$

So, the map $\mathbf{x} \mapsto w(\mathbf{x})e^{-\boldsymbol{\alpha} \cdot \mathbf{x}}$ is integrable and bounded and therefore square-integrable. It also satisfies Inequality (2.2) since it has semi-heavy tails. In conclusion, for the set δ_w , defined in Equation (3.3), it holds that $\delta_w = \mathbb{R}_-^d$. For $\lambda > 0$ and $\boldsymbol{\mu} \in \mathbb{R}^d$, let v be as in Equation (3.5). It holds for $\boldsymbol{\alpha} < \mathbf{0}$ that $\|v\|_\infty \leq \lambda^{-1}e^{-\boldsymbol{\alpha} \cdot \mathbf{y}}$ and

$$\|v\|_2^2 = \lambda^{-2} \prod_{h=1}^d \frac{\exp(-2\alpha_h(y_h))}{-2\alpha_h}.$$

Example 5.3. (A cash-or-nothing put option by the classical COS-i method). The payoff function of a cash-or-nothing put option is defined by $w(\mathbf{x}) = 1_{[0, \mathbf{K}]}(e^{\mathbf{x}})$, $\mathbf{x} \in \mathbb{R}^d$ for some $\mathbf{K} \in \mathbb{R}_+^d$; for a financial context, see Remark 4.4. The option pays 1\$ at maturity if $\mathbf{S}(T) \leq \mathbf{K}$ and nothing otherwise. The price of a cash-or-nothing put option can be approximated by the classical COS-i method as in Example 5.1 with $\mathbf{y} := \log(\mathbf{K})$ since $1_{[0, \mathbf{K}]}(e^{\mathbf{x}}) = 1_{(-\infty, \log(\mathbf{K})]}(\mathbf{x})$. In particular, the coefficients v_k of the classical COS-i method for a cash-or-nothing put option are as in Equation (5.1), replacing \mathbf{y} by $\log(\mathbf{K})$. We have that $\delta_w^\infty = \delta_w = \mathbb{R}_-^d$. According to Example 5.2, it holds that $\widehat{w}(\mathbf{z}) = \prod_{h=1}^d \frac{e^{i \log(K_h) z_h}}{iz_h}$ provided that $\Im\{z_h\} < 0$, $h = 1, \dots, d$.

Example 5.4. (L_1 -norm by the classical COS-iii method with damping). Let $w(\mathbf{x}) = \sum_{i=1}^d |x_i|$. The integral in (1.1) is equal to the expected L_1 -norm of a random variable with density g . Obtaining the L_1 -norm is a challenging numerical problem even in one dimension, see Von Bahr (1965); Brown (1972); Barndorff-Nielsen and Stelzer (2005). Note that

$$\int_{\mathbb{R}^d} w(\mathbf{x})g(\mathbf{x})d\mathbf{x} = \sum_{i=1}^d \int_{\mathbb{R}} |x|g_i(x)dx = \sum_{i=1}^d \left(\int_{\mathbb{R}} \max(x, 0)g_i(x)dx + \int_{\mathbb{R}} \max(-x, 0)g_i(x)dx \right) \quad (5.2)$$

where g_i is the i^{th} marginal density of g , which has Fourier transform $u \mapsto \widehat{g}(0, \dots, 0, u, 0, \dots, 0)$. So, the approximation of the expected L_1 -norm boils down to solving d times a one-dimensional integration problem using the middle term in (5.2). It can be solved by the classical COS-i method since $v_k = \int_{-M}^M |x| \cos(k\pi \frac{x+L}{2L}) dx$, defined in Equation (3.14), can be obtained in closed form. However, since $x \mapsto |x|$ is not bounded, Theorem 3.15 and Corollary 3.17 cannot be applied. Furthermore, the COS-i method is numerically unstable when applied to unbounded functions of interest due to significant cancellation errors, see Fang and Oosterlee (2009a, Remark 5.2). In order to solve the d -dimensional integral, i.e., the term at the left in (5.2), we propose applying the one-dimensional classical COS-iii method with damping exactly $2d$ times to approximate the term at the right in (5.2), since the functions $w_+(x) := \max(x, 0)e^{-\alpha_+ x}$ and $w_-(x) := \max(-x, 0)e^{-\alpha_- x}$ are bounded for $\alpha_+ > 0$ and $\alpha_- < 0$. For both functions, the coefficients v_k , defined in Equation (3.14), are given in closed form since $\int_M^M w_\pm(x) \cos(k\pi \frac{x+L}{2L}) dx$ can be computed explicitly. For the sets $\delta_{w_\pm}^\infty$, defined in Equation (3.2), it holds that $\delta_{w_\pm}^\infty = \mathbb{R}_\pm$.

Example 5.5. (Unweighted arithmetic basket put option by the damped COS-iv method). An unweighted arithmetic basket put option is defined by $w(\mathbf{x}) = \max(K - \sum_{h=1}^d e^{x_h}, 0)$, $\mathbf{x} \in \mathbb{R}^d$ for some $K > 0$; for

a financial context, see Remark 4.4. The Fourier transform of w exists for $\mathbf{z} \in \mathbb{C}^d$ such that $\Im\{z_h\} < 0$, $h = 1, \dots, d$, and is given by

$$\widehat{w}(\mathbf{z}) = \int_{\mathbb{R}^d} e^{i\mathbf{z}\cdot\mathbf{x}} w(\mathbf{x}) d\mathbf{x} = \frac{K^{(1+i\sum_{h=1}^d z_h)} \prod_{h=1}^d \Gamma(iz_h)}{\Gamma\left(i\sum_{h=1}^d z_h + 2\right)}. \quad (5.3)$$

Equation (5.3) follows by an elementary substitution² from Olver et al. (2010, Eq. (5.14.1)) and is also mentioned in a similar form in Hubalek and Kallsen (2003). For the set δ_w , defined in Equation (3.3), it holds that $\delta_w = \mathbb{R}_-^d$. If $\boldsymbol{\alpha} < \mathbf{0}$, it holds that $\|v\|_\infty \leq \lambda^{-1} K^{1-\sum_{h=1}^d \alpha_h}$ and, using Olver et al. (2010, Eq. (5.14.1)) once more, it follows that

$$\|v1_{[-M, M]}\|_2^2 \leq \|v\|_2^2 \leq \frac{K^{2-2\sum_{h=1}^d \alpha_h} \prod_{h=1}^d \Gamma(-2\alpha_h)}{\lambda^2 \Gamma(1 + \sum_{h=1}^d (-2\alpha_h))}.$$

There are other payoff functions with known Fourier transform which could be priced using the damped COS-iv method: For put and call options on the maximum or minimum of d assets, see Eberlein et al. (2010); for spread options, see Hurd and Zhou (2010).

6 Numerical experiments

We provide several numerical experiments to solve the integral in (1.1) using the classical COS-i or the damped COS-iv methods. Reference values are obtained by a Monte Carlo simulation as follows: Let $\varepsilon > 0$ be some error tolerance. If not stated otherwise, ε is interpreted as an absolute error tolerance. Let p be the probability that the difference between the Monte Carlo estimator with U runs and the true value of the integral is less than the error tolerance ε . Using the central limit theorem, we choose U such that $p = 0.99$. The Monte Carlo estimator is denoted by $\text{MC}(\varepsilon)$.

In all experiments, we set \mathbf{M} as in Inequality (3.28) and we set $\mathbf{L} := \mathbf{M}$. We only report \mathbf{L} . All experiments are performed on a modern laptop with Intel i7-11850H processor and 32 GB RAM. A short and pure R implementation of the classical COS-i and the damped COS-iv methods with focus on readability can be found in Algorithm 1 in the appendix. For the numerical experiments, we implemented the COS-i and COS-iv methods and the Monte Carlo simulation in C++ (this code is written with focus on performance) using for-loops without parallelization. The memory requirements are minimal and the complete code can be found in https://github.com/GeroJunike/COS_Method.

6.1 Uncertainty of the Fourier transform

We illustrate uncertainty on \widehat{f} as in Corollary 3.8, where \widehat{f} is defined by a one-dimensional ODE. An application involving multidimensional ODEs, so-called generalized Riccati equations, can be found in Duffie et al. (2003). Suppose that \widehat{f} solves the following ODE:

$$\frac{d}{du} \widehat{f}(u) = -u\widehat{f}(u), \quad u \in \mathbb{R}, \quad \widehat{f}(0) = 1. \quad (6.1)$$

The ODE can be solved numerically by the Euler method with $Q \in \mathbb{N}$ steps, where a numerical solution $\vartheta_Q : [0, \bar{u}] \rightarrow \mathbb{R}$, with $\bar{u} > 0$, is constructed as follows: for the step size $h = \frac{\bar{u}}{Q}$, set $\vartheta_Q(0) := 1$,

$$\vartheta_Q((q+1)h) := \vartheta_Q(qh) + h(-qh\vartheta_Q(qh)), \quad q = 0, \dots, Q-1,$$

and use linear interpolation in the gaps, see e.g., Griffiths and Higham (2010, Section 2). The analytic solution of the ODE (6.1) is also well known and is given by $\widehat{f}(u) = e^{-\frac{u^2}{2}}$, which is the characteristic function of a standard normal random variable. We will compare the numerical solution to the analytical

²We thank Friedrich Hubalek from Technische Universität Wien for pointing this out to us.

solution. After solving the ODE (6.1) by the Euler method, we use the classical COS-i method with ϑ_Q instead of \hat{f} to approximate $\Phi(-2) = \int_{-\infty}^{\infty} v(x)f(x)dx$, where Φ and f are the CDF and density of a standard normal random variable, respectively, and $v(x) = 1_{(-\infty, -2]}(x)$. To use the classical COS-i method, set $N = 5$ and $L = \pi$. We must approximate \hat{f} by ϑ_Q at $\mathcal{U}(L, N) = \{0, \frac{1}{2}, 1, \frac{3}{2}, 2, \frac{5}{2}\}$, compare with Equation (3.12). So we set $\bar{u} = \frac{5}{2}$. We use the error tolerance $\varepsilon = 0.0006$, which is about twice as large as the absolute difference between the classical COS-i method without uncertainty on \hat{f} and the analytical solution given by $\Phi(-2)$. Since v is bounded by 1, we set ξ in (3.20) to $\sqrt{2L}$. How can we choose Q so that the error of the COS-i method using ϑ_Q instead of \hat{f} remains below ε ? Corollary 3.8 gives a theoretical answer: We have to choose Q such that Inequality (3.24) is satisfied, i.e.,

$$\max_{u \in \mathcal{U}(L, N)} \left| \hat{f}(u) - \vartheta_Q(u) \right| \leq c := \frac{\varepsilon}{12\xi} \frac{\sqrt{L}}{\sqrt{N+1}} \approx 1.4 \times 10^{-5}.$$

Note that $\log(c) \approx -11.1$. We observe empirically from Figure 1 that for $Q \approx e^{10.5}$ Inequality (3.24) is satisfied. We also observe that the COS-i approximation then has an error of 0.00031, which is well below the error tolerance ε . For $Q \rightarrow \infty$, we see that the error of the COS-i method using ϑ_Q converges to the error of the COS-i method using \hat{f} . However, we also see in this example that $Q \approx e^{6.4}$ is already sufficient to stay below the error tolerance ε . In conclusion, we confirm empirically that if Inequality (3.24) is satisfied, the Euler approximation does not increase the error of the COS-i method too much. However, the smallest Q that keeps the error of the COS-i method below ε is about 60 times smaller than predicted by Inequality (3.24).

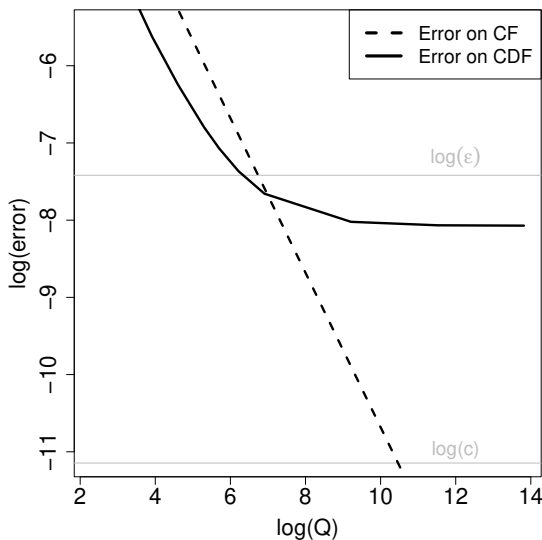


Figure 1: How the absolute error on the characteristic function (CF) propagates in the COS-i method to estimate the CDF Φ of a standard normal random variable at -2 . The solid line shows the absolute error between $\Phi(-2)$ and the COS-i method, where the characteristic function is approximated by the Euler method with Q steps. The two gray horizontal lines are the logarithmic error tolerance $\log(\varepsilon)$ and $\log(c)$.

6.2 On the choice of the damping factor and the order of convergence

We investigate the influence of the damping factor α on the accuracy of the damped COS-iv method to obtain the CDF of a multivariate normal distribution. According to Example 5.3, the CDF can also be interpreted as the price of a cash-or-nothing put option. Figure 2 shows the behavior of the damped COS-iv method for different damping factors in dimensions $d \in \{2, 3, 4\}$. If α is too close to zero, almost no damping takes place and the difference between $v_{\mathbf{k}}$ and $\tilde{v}_{\mathbf{k}}$ is large, which implies a relatively high error for the damped COS-iv method. If $|\alpha|$ is too big, $\|v\|_{\infty}$ and $\|v\|_2$ become very large and the truncation error increases.

We observe in Figure 2 that a wide range of damping factors work well in various dimensions. Fixing the number of terms \mathbf{N} and the truncation range \mathbf{L} , we see that the classical COS-i method almost always yields lower error than the damped COS-iv method, except for very specific choices for α , which can only be determined through trial and error and is not known a priori.

Table 2 shows for the multivariate normal distribution the dependence of the truncation range on the damping factor and on the correlation, i.e., on the off-diagonal elements of the covariation matrix, in $d \in \{2, 4\}$ dimensions. The truncation range does not depend on the off-diagonal elements if there is no damping. However, in the case of high correlations, large damping factors in four dimensions greatly increase the truncation range.

We also illustrate the order of convergence of the damped COS-iv method for an unweighted arithmetic basket put option in the VG model. We compare three different maturities. In Figure 2 we can see that the theoretical bound from Theorem 3.20 for the order of convergence is sharp and close to the empirical order of convergence for $T \geq 0.5$. The theoretical bound is less sharp for short maturities like $T = 0.1$.

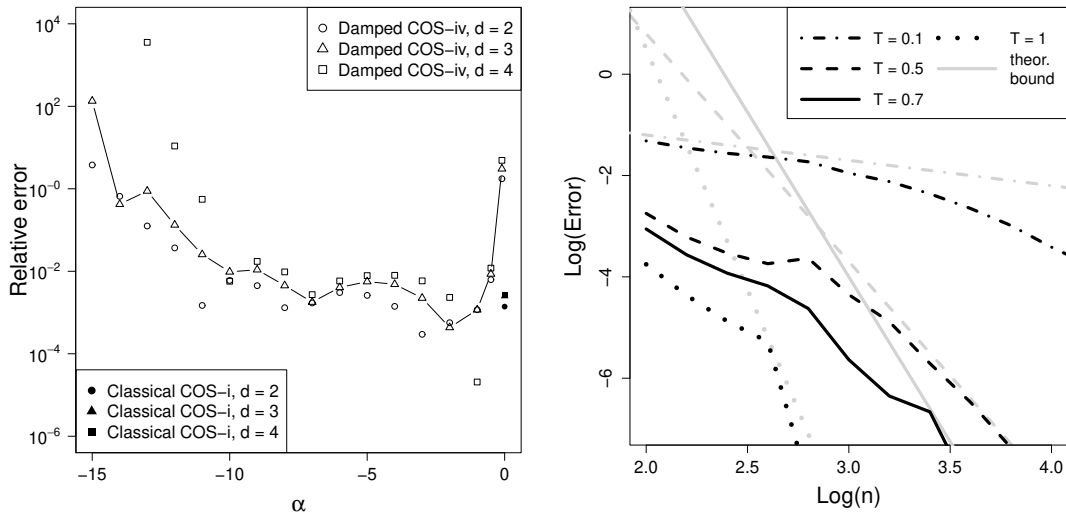


Figure 2: *Left*: Relative error of the CDF of the multivariate normal distribution with different damping factors, $\boldsymbol{\eta} = (4.58517, \dots, 4.58517)$, $\boldsymbol{y} = (4.60517, \dots, 4.60517)$ and $\Sigma_{ii} = \sigma^2$, $\Sigma_{ij} = 0.5\sigma^2$, $i \neq j$, where $\sigma = 0.2$. Further, $\mathbf{L} = (30\sigma, \dots, 30\sigma)$ and $\mathbf{N} = (60, \dots, 60)$. Reference values are obtained by a Monte Carlo $\text{MC}(10^{-5})$ simulation. *Right*: Logarithmic error of the price by the damped COS-iv method for the VG model over the logarithmic number of terms for an unweighted arithmetic basket put option and $d = 2$. We choose $\mathbf{N} = (n, n)$ and $\mathbf{L} = (\gamma n^\beta, \gamma n^\beta)$ with $\gamma = \beta = \frac{1}{2}$. We set $\mathbf{S}(0) = (50, 50)$, $K = 100$, $\boldsymbol{\sigma} = (0.2, 0.2)$, $\boldsymbol{\theta} = (-0.03, -0.03)$, $\nu = 0.1$, $r = 0$ and $\boldsymbol{\alpha} = (-4, -4)$. The theoretical bound from Theorem 3.20, i.e., a line with slope $-(1 - \beta)(p - \frac{d}{2})$, is shown in gray. For the VG model, we have $p = \frac{2T}{\nu}$. Reference values are obtained by a Monte Carlo $\text{MC}(10^{-4})$ simulation and are given by 1.6244, 3.8998, 4.6509 and 5.5951 for $T = 0.1$, $T = 0.5$, $T = 0.7$ and $T = 1$, respectively.

	$\alpha = 0$	$\alpha = -3$	$\alpha = -7$	$\alpha = -11$
$\rho = 0.00$	1.42 / 1.54	1.50 / 1.74	1.87 / 2.70	2.74 / 5.78
$\rho = 0.25$	1.42 / 1.54	1.52 / 1.86	1.99 / 3.90	3.19 / 14.32
$\rho = 0.50$	1.42 / 1.54	1.54 / 1.99	2.12 / 5.64	3.71 / 35.49
$\rho = 0.75$	1.42 / 1.54	1.55 / 2.13	2.25 / 8.14	4.31 / 87.95
$\rho = 0.99$	1.42 / 1.54	1.57 / 2.27	2.39 / 11.6	4.99 / 210.1

Table 2: Truncation ranges $\mathbf{L} = (L, \dots, L)$ for error tolerance $\varepsilon = 10^{-4}$ for a multivariate normal distribution evaluated at $\mathbf{y} = (4.60517, \dots, 4.60517)$ with location $\boldsymbol{\eta} = (4.58517, \dots, 4.58517)$ and covariance matrix $\Sigma_{ii} = \sigma^2$, $\Sigma_{ij} = \rho\sigma^2$, $i \neq j$, where $\sigma = 0.2$. We show L for the dimensions $d = 2 / d = 4$ for different values for ρ and damping factors $\boldsymbol{\alpha} = (\alpha, \dots, \alpha)$. The term L is obtained from Equation (3.28) and a bound for $|v|_\infty$ is taken from Example 5.2.

6.3 On the choice of \mathbf{N}

In this section, we approximate the CDF for the VG and the multivariate normal distributions by the classical COS-i method and the price of an unweighted arithmetic put option in the BS model by the damped COS-iv method.

We approximate the CDF for the $\text{VG}(a, s, \boldsymbol{\eta}, \boldsymbol{\theta}, \boldsymbol{\sigma})$ distribution in $d = 3$ dimensions with parameters $a = 10$, $s = 0.1$, $\boldsymbol{\eta} = \mathbf{0}$, $\boldsymbol{\theta} = (-0.03, -0.03, -0.03)$ and $\boldsymbol{\sigma} = (0.2, 0.2, 0.2)$ at 1000 different $\mathbf{y} \in \mathbb{R}^d$ by the classical COS-i method. These \mathbf{y} are randomly chosen according to the $\text{VG}(a, s, \boldsymbol{\eta}, \boldsymbol{\theta}, \boldsymbol{\sigma})$ distribution.

We set the error tolerance to $\varepsilon = 10^{-3}$ and obtain $\mathbf{L} = (1.2, 1.2, 1.2)$ using $n = 8$ moments by Inequality (3.28). The number of terms is obtained by Corollary 3.17 and is given by $\mathbf{N} = (21, 21, 21)$. We solve the integral appearing in Corollary 3.17 numerically. This takes some time, but it only has to be done once: the formulas for \mathbf{L} and \mathbf{N} depend only on the upper bound of the function of interest and not on the concrete choice of \mathbf{y} . Therefore, we use identical \mathbf{L} and \mathbf{N} for all 1000 choices for \mathbf{y} . Reference values are obtained by a Monte Carlo $\text{MC}(\frac{\varepsilon}{10})$ simulation. We observe that the error is less than ε in *all* cases. The average CPU time to compute the CDF for a single \mathbf{y} is 0.019sec. We report some \mathbf{y} corresponding to quantiles far away from the median and their COS-i approximations and reference values in Table 3. This experiment indicates that a CDF can be approximated on the entire \mathbb{R}^d by the COS-i method.

\mathbf{y}	COS-i approximation	Ref. value
(-0.49, 0.18, 0.3)	0.0103	0.0103
(-0.02, -0.02, 0.27)	0.2505	0.2505
(0.07, 0.21, 0.15)	0.5096	0.5096
(0.30, 0.26, 0.17)	0.7509	0.7508
(0.94, 0.89, 0.45)	0.9907	0.9907

Table 3: Approximation of a $\text{VG}(a, s, \boldsymbol{\eta}, \boldsymbol{\theta}, \boldsymbol{\sigma})$ distribution at different $\mathbf{y} \in \mathbb{R}^3$.

Next, we approximate the CDF for a multivariate normal distribution in $d = 4$ dimensions with location zero and covariance matrix $\Sigma_{ii} = 1$, $\Sigma_{ij} = \rho$, $i \neq j$ for $\rho = 0.75$. We set $\varepsilon = 10^{-2}$. We choose the truncation range by Inequality (3.28) and the number of terms according to Corollary 3.17. We obtain $\mathbf{L} = (4.34, \dots, 4.34)$ and $\mathbf{N} = (29, \dots, 29)$. We randomly choose 1000 different $\mathbf{y} \in \mathbb{R}^d$ according to the multivariate normal distribution with location zero and covariance matrix Σ . Then, we approximate the multivariate normal CDF at each \mathbf{y} by the classical COS-i method. The error tolerance is satisfied in *all* cases. Reference values are obtained by a Monte Carlo $\text{MC}(\frac{\varepsilon}{10})$ simulation. We repeat this experiment with other choices for ρ , i.e., $\rho \in \{0.0, 0.5, 0.9, 0.99\}$, and observe that \mathbf{L} and \mathbf{N} do not change and that the error tolerance is satisfied in all cases.

Lastly, we test the damped COS-iv method in the BS model to approximate the price of an unweighted arithmetic put option. We consider the case $d = 2$ and set $T = 1$, $r = 0$, $\mathbf{S}(0) = (50, 50)$, $K = 100$ and covariance matrix $\Sigma \in \mathbb{R}^{d \times d}$ with $\Sigma_{11} = 0.2^2$, $\Sigma_{22} = 0.4^2$, $\Sigma_{12} = \Sigma_{21} = \frac{1}{2}\sqrt{\Sigma_{11}\Sigma_{22}}$. We obtain the truncation range $\mathbf{L} = (3.9, 7.9)$ from Inequality (3.28) using $n = 8$ moments and error tolerance $\varepsilon = 10^{-2}$.

We set $\alpha = (-4, -4)$. Applying Corollary 3.17, we set $\mathbf{N} = (72, 72)$. Reference values are obtained by a Monte Carlo $\text{MC}(\frac{\varepsilon}{10})$ simulation. The damped COS-iv method prices the unweighted arithmetic put option in 0.007sec. The minimal number of terms to obtain the required error tolerance is roughly twice as large as \mathbf{N} in this example and is given by $(40, 40)$, which leads to a CPU time of 0.002sec. We average over ten runs to obtain the CPU time.

6.4 Comparison with Monte Carlo and Lewis

We compare the classical COS-i and the damped COS-iv methods with a Monte Carlo (MC) simulation in the VG and BS models to obtain the price of a digital cash-or-nothing put option or the price of an unweighted arithmetic basket put option. According to Example 5.3, the digital cash-or-nothing put option can also be interpreted as a CDF.

The computational complexity of a MC simulation with $U \in \mathbb{N}$ runs scales like $O(U)$. The classical COS-i and damped COS-iv methods consist of d -nested sums. According to Equation (3.11), the computational complexity of the COS-i and COS-iv methods scale like $O\left(\prod_{h=1}^d \{N_h\}\right)$. A MC simulation converges relatively slowly, but it scarcely depends on the dimension. On the other hand, the complexity of the COS-i and COS-iv methods grows exponentially in the dimension; however, the COS-i and COS-iv methods also converge exponentially for the multivariate normal distribution. The choice between MC and the COS method depends both on the dimension and on the error tolerance ε : the higher d , the better MC compares to the COS method, but the smaller ε , the faster the COS method performs.

In Table 4 (Table 5), we price these two options in $d \in \{2, 4\}$ dimensions in the BS model (VG model). We observe that the classical COS-i and the damped COS-iv methods in $d = 2$ dimensions are significantly faster than MC, approximately by a factor between 500 and 5000. In $d = 4$ dimensions, the COS-i method outperforms MC but the damped COS-iv method is slower than a MC simulation. The standard deviation of a single Monte Carlo run decreases in the examples discussed in Tables 4 and 5 with increasing dimension, which explains why the CPU time of the Monte Carlo method decreases as the dimension increases.

d	Function of interest	N	L	α	U	σ_{MC}	Ref. value	CPU time COS	CPU time MC
2	Cash-or-nothing put	5	0.796	0	15392	0.48	0.3741	$1.61 \cdot 10^{-5}$	0.008
4	Cash-or-nothing put	10	0.868	0	11975	0.42	0.2345	0.0072	0.01
2	Arithm. basket put	25	2.585	-3	5070844	9.16	6.9066	0.0015	1.49
4	Arithm. basket put	35	4.688	-1.5	4607857	8.38	6.3056	13.873	3.44

Table 4: Let $\varepsilon = 10^{-2}$. Comparison of a Monte Carlo $\text{MC}(\varepsilon)$ simulation to the classical COS-i method to obtain the price of a cash-or-nothing digital put option and the damped COS-iv method to obtain the price of an unweighted arithmetic basket put option in the BS model. We set $T = 1$, $r = 0$ and $\Sigma_{ii} = 0.2^2$ and $\Sigma_{ij} = \frac{1}{2} \cdot 0.2^2$ for $j \neq i$. For the cash-or-nothing put option, we set $\mathbf{S}_0 = \mathbf{K} = (100, \dots, 100)$ and for the unweighted arithmetic basket put option, we set $K = 100$ and $\mathbf{S}_0 = (\frac{100}{d}, \dots, \frac{100}{d})$. We obtain the truncation range $\mathbf{L} = (L, \dots, L)$ from Inequality (3.28) using $n = 8$ moments. The number of terms \mathbf{N} and for the basket option and the damping factor $\alpha = (\alpha, \dots, \alpha)$, are chosen, such that \mathbf{N} is minimal so that the error of the COS-i and COS-iv methods are smaller than ε . The number of runs for the Monte Carlo simulation is denoted by U . The standard deviation of a single Monte Carlo run is denoted by σ_{MC} . Reference values are calculated by a Monte Carlo $\text{MC}(\frac{\varepsilon}{10})$ simulation. We average over 10 runs to obtain the CPU time, which is measured in seconds.

d	Function of interest	N	L	α	U	σ_{MC}	Ref. value	CPU time COS	CPU time MC
2	Cash-or-nothing put	5	0.853	0	13728	0.45	0.2898	$2.79 \cdot 10^{-5}$	0.015
4	Cash-or-nothing put	5	0.930	0	5261	0.27	0.0839	0.0027	0.005
2	Arithm. basket put	20	2.581	-2.5	4002494	7.66	5.5951	0.0014	1.5
4	Arithm. basket put	30	5.029	-1.5	2133811	5.82	3.9696	16.355	1.3

Table 5: Let $\varepsilon = 10^{-2}$. Comparison of a Monte Carlo $MC(\varepsilon)$ simulation to the classical COS-i method to obtain the price of a cash-or-nothing digital put option and the damped COS-iv method to obtain the price of an unweighted arithmetic basket put option in the VG model. We set $\sigma = (0.2, \dots, 0.2)$, $\theta = (-0.03, \dots, -0.03)$, $\nu = 0.1$ and choose the other parameters as in Table 4.

We also compare the CPU time of the damped COS-iv method for very small error tolerance ε to the CPU time of a Monte Carlo simulation. For tiny ε , the computation of reference values by a Monte Carlo simulation would take too long, which is why we provide several numerical experiments with an uncorrelated multivariate normal distribution, where reference value are given in closed form. One could and should use the classical COS-i method to approximate the multivariate normal CDF, but we explicitly want to test the damped COS-iv method. We observe that the damped COS-iv method is faster than MC for $d \leq 4$ and $\varepsilon \leq 10^{-3}$. For $d = 5$, the damped COS-iv method outperforms MC for $\varepsilon \leq 10^{-5}$; otherwise, a MC simulation is faster. If $\varepsilon = 10^{-9}$ and $d = 4$, the damped COS-iv method needs 220 terms in each dimension to stay below the error tolerance and the CPU time is about one hour. We estimate that a MC simulation would take longer than 20,000 years. Some experiments are also shown in Figure 3.

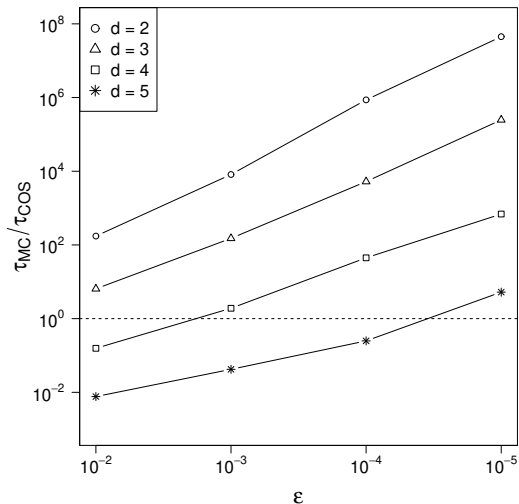


Figure 3: Ratio of the CPU time of the damped COS-iv method (τ_{COS}) and the CPU time of a MC simulation (τ_{MC}) to approximate the CDF of a multivariate normal distribution. We set $\Sigma_{ii} = \sigma^2$, $\Sigma_{ij} = 0$, $i \neq j$, where $\sigma = 0.2$, and we use $\eta = (4.58517, \dots, 4.58517)$, $\mathbf{y} = (4.60517, \dots, 4.60517)$ and $\alpha = (-7, \dots, -7)$. We obtain the truncation range $\mathbf{L} = (L, \dots, L)$ from Inequality (3.28) using $n = 8$ moments. We use the minimal number of terms \mathbf{N} to stay below the error tolerance. The reference value can be obtained in closed form.

The Lewis formula (Eberlein et al. (2010, Theorem 3.2) and Bayer et al. (2023, Proposition 2.4)) expresses the integral in (1.1) by another integral involving the Fourier-transforms \hat{g} and \hat{w} . The computational speed and robustness of the Lewis formula strongly depend on the numerical method for approximating the new integral. We implement the Lewis formula using Gauss-Hermite quadrature and the R package *mvQuad* without parallelization. Using this package, the CPU time of the Lewis formula is of the same order of magnitude as the damped COS-iv method in two dimensions and is usually faster in four dimensions, see Table 6.

d	Model	ε	Ref. value	CPU MC	CPU Lewis	CPU COS	\mathbf{L}	N	$\boldsymbol{\alpha}$	Damping Lewis
2	BS	10^{-4}	11.4474	1.7	0.003	0.001	(6.09, 6.09)	24	(-0.9, -0.9)	(2.5, 2.5)
4	BS	10^{-4}	8.193	39	0.52	48.57	(9.35, ..., 9.35)	42	(-0.7, ..., -0.7)	(2.1, ..., 2.1)
4	BS	10^{-4}	3.1	13.6	26.7	12.03	(4.57, 9.15, 13.72, 18.29)	33	(-0.9, -0.7, -0.6, -0.4)	(2.4, 1.9, 1.5, 1.2)
2	VG	10^{-3}	11.7589	16.4	0.001	0.004	(8.14, 8.14)	26	(-1, -1)	(1.7, 1.7)
4	VG	10^{-4}	8.9441	40.8	0.69	70.34	(12.80, ..., 12.80)	44	(-0.5, ..., -0.5)	(1.2, ..., 1.2)

Table 6: Comparison of the damped COS-iv method and the Lewis formula to price an unweighted arithmetic basket put option with $K = 100$, $\mathbf{S}_0 = (\frac{100}{d}, \dots, \frac{100}{d})$, $T = 1$ and $r = 0$. Reference values, optimal damping factors for the Lewis formula and number of runs for the Monte Carlo simulation are taken from Bayer et al. (2023, Tab. 4.6), who used the following parameters for the BS model: $\Sigma_{ii} = 0.4^2$ (first two rows), $\Sigma_{ii} = (\frac{2i}{10})^2$ (third row) and $\Sigma_{ij} = 0$, $i \neq j$. For the VG model, they set $\boldsymbol{\sigma} = (0.4, \dots, 0.4)$, $\boldsymbol{\theta} = (-0.3, \dots, -0.3)$ and $\nu = 0.257$. We obtain the truncation range \mathbf{L} for the COS-iv method from Inequality (3.28) using $n = 8$ moments and setting the absolute error tolerance ε (approximately) equal to the statistical error of the reference values taken from Bayer et al. (2023, Table 4.1). The number of terms $\mathbf{N} = (N, \dots, N)$ and the damping factor $\boldsymbol{\alpha}$ are chosen so that \mathbf{N} is minimal and the relative errors of the COS-iv method are smaller or equal to the relative errors of the Lewis formula, which are of the order 10^{-4} . We average over 10 runs to obtain the CPU time, which is measured in seconds.

7 Conclusion

In this article we introduced and discussed in general dimensions the classical and the damped COS methods, which are tools for solving certain multidimensional integrals numerically, e.g., approximating the CDF from a characteristic function or pricing a financial contract. We showed that the classical and the damped COS methods converge exponentially if the Fourier transform of the (damped) density decays exponentially.

We compared the classical and the damped COS methods to other numerical techniques, such as the Lewis formula and Monte Carlo simulations. In terms for speed, we observed that the classical and damped COS methods are faster than a crude Monte Carlo simulation in two and three dimensions but slower in five dimensions for an absolute error tolerance of about 10^{-2} . The choice between the COS method and a Monte Carlo simulation in four dimensions depends on the required error tolerance and the function of interest.

The Lewis formula requires solving an integral involving the Fourier transforms of the density and the function of interest numerically. The computational speed of the Lewis formula depends strongly on the numerical method used to solve that integral. In our experiments, the CPU time of the Lewis formula is of the same order of magnitude as the damped COS-iv method in two dimensions and usually faster in four dimensions.

Let us compare the three methods in terms of error control: The number of runs for a crude Monte Carlo simulation is given explicitly thanks to the central limit theorem. The classical COS method requires two parameters: a truncation range and a number of terms. We developed explicit and implicit formulas for both parameters. A damping parameter needs to be provided to apply the damped COS method. So far, we are only able to find the damping factor by trial and error. The Lewis formula also requires a damping factor, which can be obtained via an optimization techniques, see Bayer et al. (2023). However, the Lewis formula requires a numerical integration method and hence some tuning parameters such as a number of quadrature points, etc., which are not always easy to estimate.

Acknowledgments

We thank two anonymous referees for very helpful comments that improved this paper.

Declarations

The authors declare no competing interests.

Availability of data, materials and Code

No data was used for the research described in the article. The code for the experiments presented in this paper is available online. URLs are included in this article.

A Auxiliary results

Proposition A.1. *Assume $\psi \in \mathcal{L}^1 \cap \mathcal{L}^2$. Then ψ is COS-admissible if Inequality (2.2) holds. Let $\mathbf{L} = (L_1, \dots, L_d) \in \mathbb{R}_+^d$; then it holds that*

$$B_\psi(\mathbf{L}) \leq \Xi \int_{\mathbb{R}^d \setminus [-\mathbf{L}, \mathbf{L}]} \prod_{h=1}^d \max\{x_h^2 L_h^{-2}, 1\} |\psi(\mathbf{x})|^2 d\mathbf{x} \quad (\text{A.1})$$

$$\leq \frac{\Xi}{d \min_{h=1, \dots, d} L_h^{2d}} \int_{\mathbb{R}^d \setminus [-\mathbf{L}, \mathbf{L}]} |\mathbf{x}|^{2d} |\psi(\mathbf{x})|^2 d\mathbf{x} + \Xi \int_{\mathbb{R}^d \setminus [-\mathbf{L}, \mathbf{L}]} |\psi(\mathbf{x})|^2 d\mathbf{x}, \quad (\text{A.2})$$

where $\Xi = \frac{\pi^2}{3} \sum_{h=1}^d \left(\frac{\pi^2}{3} + 1\right)^{h-1}$.

Proof. Let $\mathbf{L} \in \mathbb{R}_+^d$ and $\mathbf{j} \in \mathbb{Z}^d$. It follows by Parseval's identity

$$\begin{aligned} \int_{[2\mathbf{j}\mathbf{L}-\mathbf{L}, 2\mathbf{j}\mathbf{L}+\mathbf{L}]} |\psi(\mathbf{x})|^2 d\mathbf{x} &= \sum'_{\mathbf{k} \in \mathbb{N}_0^d} \frac{1}{\prod_{h=1}^d L_h} \left| \int_{[2\mathbf{j}\mathbf{L}-\mathbf{L}, 2\mathbf{j}\mathbf{L}+\mathbf{L}]} \psi(\mathbf{x}) \prod_{h=1}^d \underbrace{\cos\left(k_h \pi \frac{x_h - (2j_h L_h - L_h)}{2L_h}\right)}_{=(-1)^{j_h k_h} \cos\left(k_h \pi \frac{x_h + L_h}{2L_h}\right)} d\mathbf{x} \right|^2 \\ &= \sum'_{\mathbf{k} \in \mathbb{N}_0^d} \frac{1}{\prod_{h=1}^d L_h} \left| \int_{[2\mathbf{j}\mathbf{L}-\mathbf{L}, 2\mathbf{j}\mathbf{L}+\mathbf{L}]} \psi(\mathbf{x}) e_{\mathbf{k}}(\mathbf{x}) d\mathbf{x} \right|^2. \end{aligned} \quad (\text{A.3})$$

By the Cauchy-Schwarz inequality, we obtain with $\varrho(\mathbf{j}) := \prod_{h=1}^d \max\{|j_h|, 1\}$,

$$\begin{aligned} \left| \int_{\mathbb{R}^d \setminus [-\mathbf{L}, \mathbf{L}]} \psi(\mathbf{x}) e_{\mathbf{k}}(\mathbf{x}) d\mathbf{x} \right|^2 &= \left| \sum_{\mathbf{j} \in \mathbb{Z}^d \setminus \{\mathbf{0}\}} \frac{\varrho(\mathbf{j})}{\varrho(\mathbf{j})} \int_{[2\mathbf{j}\mathbf{L}-\mathbf{L}, 2\mathbf{j}\mathbf{L}+\mathbf{L}]} \psi(\mathbf{x}) e_{\mathbf{k}}(\mathbf{x}) d\mathbf{x} \right|^2 \\ &\leq \underbrace{\left(\sum_{\mathbf{j} \in \mathbb{Z}^d \setminus \{\mathbf{0}\}} \frac{1}{(\varrho(\mathbf{j}))^2} \right)}_{=\Xi} \sum_{\mathbf{j} \in \mathbb{Z}^d \setminus \{\mathbf{0}\}} (\varrho(\mathbf{j}))^2 \left| \int_{[2\mathbf{j}\mathbf{L}-\mathbf{L}, 2\mathbf{j}\mathbf{L}+\mathbf{L}]} \psi(\mathbf{x}) e_{\mathbf{k}}(\mathbf{x}) d\mathbf{x} \right|^2. \end{aligned} \quad (\text{A.4})$$

The fact that $\Xi = \frac{\pi^2}{3} \sum_{h=1}^d \left(\frac{\pi^2}{3} + 1\right)^{h-1}$ can be shown by mathematical induction over d . Then it follows that

$$\begin{aligned} B_\psi(\mathbf{L}) &\stackrel{(\text{A.4})}{\leq} \sum_{\mathbf{j} \in \mathbb{Z}^d \setminus \{\mathbf{0}\}} (\varrho(\mathbf{j}))^2 \sum'_{\mathbf{k} \in \mathbb{N}_0^d} \frac{1}{\prod_{h=1}^d L_h} \left| \int_{[2\mathbf{j}\mathbf{L}-\mathbf{L}, 2\mathbf{j}\mathbf{L}+\mathbf{L}]} \psi(\mathbf{x}) e_{\mathbf{k}}(\mathbf{x}) d\mathbf{x} \right|^2 \\ &\stackrel{(\text{A.3})}{=} \sum_{\mathbf{j} \in \mathbb{Z}^d \setminus \{\mathbf{0}\}} (\varrho(\mathbf{j}))^2 \int_{[2\mathbf{j}\mathbf{L}-\mathbf{L}, 2\mathbf{j}\mathbf{L}+\mathbf{L}]} |\psi(\mathbf{x})|^2 d\mathbf{x}. \end{aligned}$$

For $\mathbf{j} \in \mathbb{Z}^d$ and $\mathbf{x} \in [2\mathbf{j}\mathbf{L} - \mathbf{L}, 2\mathbf{j}\mathbf{L} + \mathbf{L}]$, one has $|j_h| \leq \frac{|\mathbf{x}_h|}{L_h}$, $h = 1, \dots, d$. It follows that $(\varrho(\mathbf{j}))^2 \leq \prod_{h=1}^d \max\{x_h^2 L_h^{-2}, 1\}$, which implies Inequality (A.1). By Young's inequality, it holds that

$$\prod_{h=1}^d (\max\{x_h^2 L_h^{-2}, 1\})^{\frac{1}{2}} \leq \frac{1}{d} \sum_{h=1}^d \max\{x_h^2 L_h^{-2}, 1\} \leq \frac{|\mathbf{x}|^{2d}}{d \min_{h=1, \dots, d} L_h^{2d}} + 1.$$

In the last inequality, we used $\max\{a, b\} \leq a + b$ for any $a, b \geq 0$ and $\sum_{h=1}^d x_h^{2d} \leq |\mathbf{x}|^{2d}$, which follows from the monotonicity of the p -norm. Hence, Inequality (A.2) holds. Assumption (2.2) and $\psi \in \mathcal{L}^2$ imply $B_\psi(\mathbf{L}) \rightarrow 0$, $\min_{h=1, \dots, d} L_h \rightarrow \infty$. \square

Proposition A.2. *Let $\boldsymbol{\alpha} \in \mathbb{R}^d$. Assume that g is a density and that $\mathbf{x} \mapsto |\mathbf{x}|e^{\boldsymbol{\alpha}\cdot\mathbf{x}}g(\mathbf{x})$ is integrable. Let $\lambda = (\widehat{g}(-i\boldsymbol{\alpha}))^{-1}$ then $\lambda \in (0, \infty)$. Choose $\boldsymbol{\mu} \in \mathbb{R}^d$ by*

$$\mu_h = -\lambda i \left. \frac{\partial}{\partial u_h} \widehat{g}(\mathbf{u} - i\boldsymbol{\alpha}) \right|_{\mathbf{u}=\mathbf{0}}, \quad h = 1, \dots, d. \quad (\text{A.5})$$

Define f as in Equation (3.4). Then f is a density with characteristic function

$$\widehat{f}(\mathbf{u}) = \lambda e^{-i\mathbf{u}\cdot\boldsymbol{\mu}} \widehat{g}(\mathbf{u} - i\boldsymbol{\alpha}), \quad \mathbf{u} \in \mathbb{R}^d. \quad (\text{A.6})$$

Further, the moments of f of first order are zero, i.e., $\int_{\mathbb{R}^d} f(\mathbf{x})x_h d\mathbf{x} = 0$, $h = 1, \dots, d$.

Proof. Use $\int |\mathbf{x}|e^{\boldsymbol{\alpha}\cdot\mathbf{x}}g(\mathbf{x})d\mathbf{x} < \infty$ and split the integration range into $\mathbb{R}^d \setminus B_1$ and B_1 , where B_1 is the unit ball, to see that $\mathbf{x} \mapsto e^{\boldsymbol{\alpha}\cdot\mathbf{x}}g(\mathbf{x})$ is integrable. Since $\lambda = (\int_{\mathbb{R}^d} e^{\boldsymbol{\alpha}\cdot\mathbf{x}}g(\mathbf{x})d\mathbf{x})^{-1}$ and g is a density we have $\lambda \in (0, \infty)$. By the definition of λ , f is a density. Since $f \in \mathcal{L}^1$, \widehat{f} exists. Note that

$$\widehat{f}(\mathbf{u}) = \int_{\mathbb{R}^d} \lambda e^{\boldsymbol{\alpha}\cdot(\mathbf{x}+\boldsymbol{\mu})} g(\mathbf{x} + \boldsymbol{\mu}) e^{i\mathbf{u}\cdot\mathbf{x}} d\mathbf{x} = \lambda \int_{\mathbb{R}^d} e^{\boldsymbol{\alpha}\cdot\mathbf{x}} g(\mathbf{x}) e^{i\mathbf{u}\cdot(\mathbf{x}-\boldsymbol{\mu})} d\mathbf{x} = \lambda e^{-i\boldsymbol{\mu}\cdot\mathbf{u}} \int_{\mathbb{R}^d} g(\mathbf{x}) e^{i(\mathbf{u}-i\boldsymbol{\alpha})\cdot\mathbf{x}} d\mathbf{x},$$

which implies Equation (A.6). By Bauer (1996, Thm 25.2), the partial derivatives in Equation (A.5) exist and it holds that $\mu_h = \lambda \int_{\mathbb{R}^d} e^{\boldsymbol{\alpha}\cdot\mathbf{x}} g(\mathbf{x}) x_h d\mathbf{x}$. Finally, we have that

$$\int_{\mathbb{R}^d} f(\mathbf{x})x_h d\mathbf{x} = \int_{\mathbb{R}^d} \lambda e^{\boldsymbol{\alpha}\cdot(\mathbf{x}+\boldsymbol{\mu})} g(\mathbf{x} + \boldsymbol{\mu}) x_h d\mathbf{x} = \lambda \int_{\mathbb{R}^d} e^{\boldsymbol{\alpha}\cdot\mathbf{x}} g(\mathbf{x}) x_h d\mathbf{x} - \mu_h \lambda \int_{\mathbb{R}^d} e^{\boldsymbol{\alpha}\cdot\mathbf{x}} g(\mathbf{x}) d\mathbf{x} = 0.$$

\square

Lemma A.3. *Let $\psi \in \mathcal{L}^1 \cap \mathcal{L}^2$. Let $\mathbf{M}, \mathbf{L} \in \mathbb{R}_+^d$ with $\mathbf{M} \leq \mathbf{L}$; then it holds that*

$$\|\psi 1_{[-\mathbf{L}, \mathbf{L}]} - \sum'_{\mathbf{0} \leq \mathbf{k} \leq \mathbf{N}} a_{\mathbf{k}} e_{\mathbf{k}} 1_{[-\mathbf{L}, \mathbf{L}]} \|_2^2 \leq \int_{\mathbb{R}^d} |\psi(\mathbf{x})|^2 d\mathbf{x} - \prod_{h=1}^d L_h \sum'_{\mathbf{0} \leq \mathbf{k} \leq \mathbf{N}} |c_{\mathbf{k}}|^2 + G(\mathbf{L}),$$

where

$$G(\mathbf{L}) := B_\psi(\mathbf{L}) + 2 \sqrt{B_\psi(\mathbf{L}) \int_{\mathbb{R}^d} |\psi(\mathbf{x})|^2 d\mathbf{x}}. \quad (\text{A.7})$$

Proof. Let

$$\phi_{\mathbf{k}} := \frac{1}{\prod_{h=1}^d L_h} \int_{\mathbb{R}^d \setminus [-\mathbf{L}, \mathbf{L}]} \psi(\mathbf{x}) e_{\mathbf{k}}(\mathbf{x}) d\mathbf{x}, \quad \mathbf{k} \in \mathbb{N}_0^d.$$

It holds that $c_{\mathbf{k}} = a_{\mathbf{k}} + \phi_{\mathbf{k}}$. It follows by the Cauchy-Schwarz inequality that

$$\begin{aligned}
\prod_{h=1}^d L_h \sum'_{\mathbf{0} \leq \mathbf{k} \leq \mathbf{N}} |c_{\mathbf{k}}|^2 &= \prod_{h=1}^d L_h \left(\sum'_{\mathbf{0} \leq \mathbf{k} \leq \mathbf{N}} |a_{\mathbf{k}}|^2 + \sum'_{\mathbf{0} \leq \mathbf{k} \leq \mathbf{N}} |\phi_{\mathbf{k}}|^2 + 2 \sum'_{\mathbf{0} \leq \mathbf{k} \leq \mathbf{N}} |\phi_{\mathbf{k}}| |a_{\mathbf{k}}| \right) \\
&\leq \prod_{h=1}^d L_h \sum'_{\mathbf{0} \leq \mathbf{k} \leq \mathbf{N}} |a_{\mathbf{k}}|^2 + B_{\psi}(\mathbf{L}) + 2 \prod_{h=1}^d L_h \sqrt{\sum'_{\mathbf{0} \leq \mathbf{k} \leq \mathbf{N}} |\phi_{\mathbf{k}}|^2 \sum'_{\mathbf{0} \leq \mathbf{k} \leq \mathbf{N}} |a_{\mathbf{k}}|^2} \\
&\stackrel{(A.3)}{\leq} \prod_{h=1}^d L_h \sum'_{\mathbf{0} \leq \mathbf{k} \leq \mathbf{N}} |a_{\mathbf{k}}|^2 + \underbrace{B_{\psi}(\mathbf{L}) + 2 \sqrt{B_{\psi}(\mathbf{L}) \int_{\mathbb{R}^d} |\psi(\mathbf{x})|^2 d\mathbf{x}}}_{=G(\mathbf{L})} \tag{A.8}
\end{aligned}$$

$$\stackrel{(A.3)}{\leq} \int_{\mathbb{R}^d} |\psi(\mathbf{x})|^2 d\mathbf{x} + G(\mathbf{L}). \tag{A.9}$$

Hence,

$$\begin{aligned}
\|\psi 1_{[-L, L]} - \sum'_{\mathbf{0} \leq \mathbf{k} \leq \mathbf{N}} a_{\mathbf{k}} e_{\mathbf{k}} 1_{[-L, L]}\|_2^2 &\stackrel{(3.18)}{\leq} \prod_{h=1}^d L_h \sum'_{k_1 > N_1 \text{ or } \dots \text{ or } k_d > N_d} |a_{\mathbf{k}}|^2 \\
&= \prod_{h=1}^d L_h \sum'_{\mathbf{k} \in \mathbb{N}_0^d} |a_{\mathbf{k}}|^2 - \prod_{h=1}^d L_h \sum'_{\mathbf{0} \leq \mathbf{k} \leq \mathbf{N}} |a_{\mathbf{k}}|^2 \\
&\stackrel{(A.3, A.8)}{\leq} \int_{\mathbb{R}^d} |\psi(\mathbf{x})|^2 d\mathbf{x} - \prod_{h=1}^d L_h \sum'_{\mathbf{0} \leq \mathbf{k} \leq \mathbf{N}} |c_{\mathbf{k}}|^2 + G(\mathbf{L}).
\end{aligned}$$

□

A R code and pseudocode

Algorithm 1 Pure R code for the classical COS-i and the damped COS-iv methods to obtain the CDF at $\mathbf{y} = (1.5, 1.5)$ of a two dimensional normal distribution with location $\boldsymbol{\eta} = (-1, 0)$ and covariance matrix Σ with $\Sigma_{11} = 1$, $\Sigma_{22} = 4$, $\Sigma_{12} = \Sigma_{21} = 0.7$.

```

d = 2
y = c(1.5, 1.5)
Sigma = matrix(c(1.0, 0.7, 0.7, 4.0), nrow = d)
eta = c(-1.0, 0)
N = c(40, 40)    #N can be estimated using Alg. 2
eps = 10^-3
lambda = function(alpha){exp(-sum(eta * alpha) - 0.5 * sum(alpha * Sigma %*% alpha))}    #Exa. 4.1
mu_8 = 105 * diag(Sigma)^4    #8th marginal moments, Eq. (3.27)
v_inf_norm = function(alpha){1 / lambda(alpha) * exp(-sum(alpha * y))}    #See Exa. 5.2
M = function(alpha) (3 * d / eps * v_inf_norm(alpha) * mu_8)^(1 / 8)    #Eq. (3.28)
L = function(alpha){M(alpha)}
mu = function(alpha){eta + Sigma %*% alpha}    #Exa. 4.1
fhat = function(u){exp(-0.5 * sum(u * Sigma %*% u))}    #Exa. 4.1
tmp = function(s, k, psi){Re(psi(pi / 2 * s * k / L(alpha)) * exp(li * pi / 2 * sum(s * k)))}    #addend for Eq. (3.11, 3.16)

##### CLASSICAL COS-i METHOD#####
classical_COS_CDF = 0
alpha = rep(0,d)    #Damping factor
for(k1 in 0:N[1]){
  for(k2 in 0:N[2]){
    k = c(k1, k2)
    ck = 1 / (2^(d - 1) * prod(L(alpha))) * (tmp(c(1, 1), k, fhat) + tmp(c(1, -1), k, fhat))    #Eq. (3.11)
    A = pmin(y - mu(rep(0, d)), M(alpha))    #Exa. 5.1
    tmp_variable = (sin(k[k != 0] * pi * (A[k != 0] + L(alpha)[k != 0]) / (2 * L(alpha)[k != 0])))    #Using that M = L
    vk = prod(A[k == 0] + M(alpha)[k == 0]) * prod(2 * L(alpha)[k != 0] / (k[k != 0] * pi) * tmp_variable) #Eq. (5.1)
    if(any((y - mu(rep(0, d))) < -M(alpha)))
      vk = 0
    classical_COS_CDF = classical_COS_CDF + 1 / (2^sum(k == 0)) * ck * vk    #Eq. (3.14)
  }
}
classical_COS_CDF    #0.7708859

##### DAMPED COS-iv METHOD#####
what = function(z){prod(exp(li * y * z) / (li * z))}    #Exa. 5.2
vhat = function(u){1 / lambda(alpha) * exp(-li * sum(u * mu(alpha))) * what(u + li * alpha)}    #Rem. 3.1
damped_COS_CDF = 0
alpha = rep(-1.0, d)    #Damping factor
for(k1 in 0:N[1]){
  for(k2 in 0:N[2]){
    k = c(k1, k2)
    ck = 1 / (2^(d - 1) * prod(L(alpha))) * (tmp(c(1, 1), k, fhat) + tmp(c(1, -1), k, fhat))    #Eq. (3.11)
    vk_tilde = 1 / (2^(d - 1)) * (tmp(c(1, 1), k, vhat) + tmp(c(1, -1), k, vhat))    #Eq. (3.16)
    damped_COS_CDF = damped_COS_CDF + 1 / (2^sum(k == 0)) * ck * vk_tilde    #Eq. (3.15)
  }
}
damped_COS_CDF    #0.7708836

```

Algorithm 2 Approximate $\int_{\mathbb{R}^d} v(\mathbf{x})f(\mathbf{x})d\mathbf{x}$ by the classical COS-i method, i.e., the sum $\sum'_{\mathbf{0} \leq \mathbf{k} \leq N} c_{\mathbf{k}}v_{\mathbf{k}}$. To apply the damped COS-iv method, replace $v_{\mathbf{k}}$ by $\tilde{v}_{\mathbf{k}}$ defined in Equation (3.16). The number of terms N can be found during the evaluation of the sum by Inequality (3.31). The function Λ is defined in Section 2.

Input: Error tolerance $\varepsilon > 0$ and the real number $I := (2\pi)^{-d} \int_{\mathbb{R}^d} |\hat{f}(\mathbf{u})|^2 d\mathbf{u}$.

Output: Approximation of $\int_{\mathbb{R}^d} v(\mathbf{x})f(\mathbf{x})d\mathbf{x}$ within the error tolerance ε .

```

DEFINE  $L, M$  via Eq. (3.28)

DEFINE  $c_{\mathbf{k}}$  via Eq. (3.11)

DEFINE  $v_{\mathbf{k}}$  via Eq. (3.14)

SET  $\mathbf{k} := \mathbf{0} \in \mathbb{N}_0^d, N := \mathbf{0} \in \mathbb{N}_0^d, \gamma := 2^{-\Lambda(\mathbf{k})}|c_{\mathbf{k}}|^2$  and  $\beta := 2^{-\Lambda(\mathbf{k})}c_{\mathbf{k}}v_{\mathbf{k}}$ 

WHILE  $\left| I - \gamma \prod_{h=1}^d L_h \right| > \frac{\varepsilon^2}{162\|v\|_2^2}$  DO:
    FOR  $\mathbf{k} \in \{\mathbf{0} \leq \mathbf{u} \leq N + \mathbf{1}\} \setminus \{\mathbf{0} \leq \mathbf{u} \leq N\}$  DO:
        SET  $\gamma := \gamma + 2^{-\Lambda(\mathbf{k})}|c_{\mathbf{k}}|^2$ 
        SET  $\beta := \beta + 2^{-\Lambda(\mathbf{k})}c_{\mathbf{k}}v_{\mathbf{k}}$ 
    INCREMENT  $N_h, h = 1, \dots, d$ , by 1
RETURN  $\beta$ 

```

References

- M. Abramowitz and I. A. Stegun. *Handbook of mathematical functions with formulas, graphs, and mathematical tables*, volume 55. US Government printing office, 1972.
- H. Amann and J. Escher. *Analysis III*. Birkhäuser Verlag AG, Springer, 2009.
- K. Andersson, A. Andersson, and C. W. Oosterlee. Convergence of a robust deep FBSDE method for stochastic control. *SIAM Journal on Scientific Computing*, 45(1):A226–A255, 2023.
- C. Bardgett, E. Gourier, and M. Leippold. Inferring volatility dynamics and risk premia from the S&P 500 and VIX markets. *Journal of Financial Economics*, 131(3):593–618, 2019.
- O. E. Barndorff-Nielsen. Normal inverse Gaussian distributions and stochastic volatility modelling. *Scandinavian Journal of Statistics*, 24(1):1–13, 1997.
- O. E. Barndorff-Nielsen and R. Stelzer. Absolute moments of generalized hyperbolic distributions and approximate scaling of normal inverse Gaussian Lévy processes. *Scandinavian Journal of Statistics*, 32(4):617–637, 2005.
- Fabio Baschetti, Giacomo Bormetti, Silvia Romagnoli, and Pietro Rossi. The SINC way: A fast and accurate approach to Fourier pricing. *Quantitative Finance*, 22(3):427–446, 2022.
- H. Bauer. *Probability Theory*, volume 23. Walter de Gruyter, 1996.
- C. Bayer, C. B. Hammouda, A. Papapantoleon, M. Samet, and R. Tempone. Optimal Damping with Hierarchical Adaptive Quadrature for Efficient Fourier Pricing of Multi-Asset Options in Lévy Models. *Journal of Computational Finance*, 27(3):43–86, 2023.
- Christian Bayer, Chiheb Ben Hammouda, Antonis Papapantoleon, Michael Samet, and Raul Tempone. Quasi-Monte Carlo for Efficient Fourier Pricing of Multi-Asset Options. *arXiv preprint arXiv:2403.02832*, 2024.

- B. M. Brown. Formulae for absolute moments. *Journal of the Australian Mathematical Society*, 13(1):104–106, 1972.
- P. Carr and D. Madan. Option valuation using the fast Fourier transform. *Journal of Computational Finance*, 2(4):61–73, 1999.
- D. Duffie, D. Filipović, and W. Schachermayer. Affine processes and applications in finance. *The Annals of Applied Probability*, 13(3):984–1053, 2003.
- E. Eberlein, K. Glau, and A. Papapantoleon. Analysis of Fourier transform valuation formulas and applications. *Applied Mathematical Finance*, 17(3):211–240, 2010.
- F. Fang and C. W. Oosterlee. A novel pricing method for European options based on Fourier-cosine series expansions. *SIAM Journal on Scientific Computing*, 31(2):826–848, 2009a.
- F. Fang and C. W. Oosterlee. Pricing early-exercise and discrete barrier options by Fourier-cosine series expansions. *Numerische Mathematik*, 114(1):27, 2009b.
- F. Fang and C. W. Oosterlee. A Fourier-based valuation method for Bermudan and barrier options under Heston’s model. *SIAM Journal on Financial Mathematics*, 2(1):439–463, 2011.
- J. Gil-Pelaez. Note on the inversion theorem. *Biometrika*, 38(3-4):481–482, 1951.
- David Francis Griffiths and Desmond J Higham. *Numerical methods for ordinary differential equations: initial value problems*, volume 5. Springer, 2010.
- L. A. Grzelak and C. W. Oosterlee. On the Heston model with stochastic interest rates. *SIAM Journal on Financial Mathematics*, 2(1):255–286, 2011.
- F. Hubalek and J. Kallsen. Variance-optimal hedging and Markowitz-efficient portfolios for multivariate processes with stationary independent increments with and without constraints. *TU München*, 2003.
- P. Hughett. Error bounds for numerical inversion of a probability characteristic function. *SIAM journal on numerical analysis*, 35(4):1368–1392, 1998.
- T. R. Hurd and Z. Zhou. A Fourier transform method for spread option pricing. *SIAM Journal on Financial Mathematics*, 1(1):142–157, 2010.
- G. Junike. On the number of terms in the COS method for European option pricing. *Numerische Mathematik*, 2024.
- G. Junike and K. Pankrashkin. Precise option pricing by the COS method—How to choose the truncation range. *Applied Mathematics and Computation*, 421:126935, 2022.
- J Lars Kirkby. Efficient option pricing by frame duality with the fast Fourier transform. *SIAM Journal on Financial Mathematics*, 6(1):713–747, 2015.
- U. Küchler and S. Tappe. On the shapes of bilateral Gamma densities. *Statistics & Probability Letters*, 78(15):2478–2484, 2008.
- Á. Leitao, C. W. Oosterlee, L. Ortiz-Gracia, and S. M. Bohte. On the data-driven COS method. *Applied Mathematics and Computation*, 317:68–84, 2018.
- Alan L Lewis. A simple option formula for general jump-diffusion and other exponential Lévy processes. *Available at SSRN 282110*, 2001.
- S. Liu, A. Borovykh, L. A. Grzelak, and C. W. Oosterlee. A neural network-based framework for financial model calibration. *Journal of Mathematics in Industry*, 9:1–28, 2019a.
- S. Liu, C. W. Oosterlee, and S. M. Bohte. Pricing options and computing implied volatilities using neural networks. *Risks*, 7(1):16, 2019b.

- R. Lord, F. Fang, F. Bervoets, and C. W. Oosterlee. A fast and accurate FFT-based method for pricing early-exercise options under Lévy processes. *SIAM Journal on Scientific Computing*, 30(4):1678–1705, 2008.
- E. Luciano and W. Schoutens. A multivariate jump-driven financial asset model. *Quantitative finance*, 6(5):385–402, 2006.
- D. Madan, P. P. Carr, and E. C. Chang. The Variance Gamma process and Option Pricing. *Review of Finance*, 2(1):79–105, 1998.
- F. W. J. Olver, D. W. Lozier, R. F. Boisvert, and C. W. Clark. *NIST handbook of mathematical functions*. Cambridge university press, 2010.
- C. W. Oosterlee and L. A. Grzelak. *Mathematical modeling and computation in finance: with exercises and Python and MATLAB computer codes*. World Scientific, 2019.
- L. Ortiz-Gracia and C. W. Oosterlee. Robust pricing of European options with wavelets and the characteristic function. *SIAM Journal on Scientific Computing*, 35(5):B1055–B1084, 2013.
- L. Ortiz-Gracia and C. W. Oosterlee. A highly efficient Shannon wavelet inverse Fourier technique for pricing European options. *SIAM Journal on Scientific Computing*, 38(1):B118–B143, 2016.
- Marcus Pivato. *Linear partial differential equations and Fourier theory*. Cambridge University Press, 2010.
- M. J. Ruijter and C. W. Oosterlee. Two-dimensional Fourier cosine series expansion method for pricing financial options. *SIAM Journal on Scientific Computing*, 34(5):B642–B671, 2012.
- M. J. Ruijter and C. W. Oosterlee. A Fourier cosine method for an efficient computation of solutions to BSDEs. *SIAM Journal on Scientific Computing*, 37(2):A859–A889, 2015.
- B. Schorr. Numerical inversion of a class of characteristic functions. *BIT Numerical Mathematics*, 15(1):94–102, 1975.
- W. Schoutens. *Lévy Processes in Finance: Pricing Financial Derivatives*. Wiley Online Library, 2003.
- N. G. Shephard. From characteristic function to distribution function: a simple framework for the theory. *Econometric theory*, 7(4):519–529, 1991a.
- N. G. Shephard. Numerical integration rules for multivariate inversions. *Journal of Statistical Computation and Simulation*, 39(1-2):37–46, 1991b.
- B. Von Bahr. On the convergence of moments in the central limit theorem. *The Annals of Mathematical Statistics*, pages 808–818, 1965.
- L. A. Waller, B. W. Turnbull, and J. M. Hardin. Obtaining distribution functions by numerical inversion of characteristic functions with applications. *The American Statistician*, 49(4):346–350, 1995.
- Chunfa Wang. Pricing European Options by Stable Fourier-Cosine Series Expansions. *arXiv preprint arXiv:1701.00886*, 2017.
- B. Zhang and C. W. Oosterlee. Efficient pricing of European-style Asian options under exponential Lévy processes based on Fourier cosine expansions. *SIAM Journal on Financial Mathematics*, 4(1):399–426, 2013.